2018

Thermomagnetic Convective Cooling of Hall Effect Thruster

Elizabeth M. Vanheusden
Michigan Technological University, emvanheu@mtu.edu

THERMOMAGNETIC CONVECTIVE COOLING OF HALL EFFECT THRUSTER

By

Elizabeth M. Van Heusden

A THESIS

Submitted in partial fulfillment of the requirements for the degree of

MASTER OF SCIENCE

In Mechanical Engineering

MICHIGAN TECHNOLOGICAL UNIVERSITY

2018

This thesis has been approved in partial fulfillment of the requirements for the Degree of MASTER OF SCIENCE in Mechanical Engineering.

Department of Mechanical Engineering – Engineering Mechanics

Thesis Advisor:	*Dr. Lyon B. King*
Committee Member:	*Dr. Jason Sommerville*
Committee Member:	*Dr. Chunpei Cai*
Department Chair:	*Dr. William Predebon*

Table of Contents

List of Figures

List of Tables

Acknowledgements

Every journey starts with an idea. God has been a critical part of this journey, He sent me on this long before I even had the idea for this journey and I have learn so much more about Him through this adventure.

Motivators and encouragers are also an important part of any journey. I would like to thank my advisor, Dr. Lyon B. King, for all his support and faith in me after taking a nine-year break from doing anything science or engineering related.

Friends that are also on the same journey play an important part of keeping you the journey. I would like to thank the members of the ISP lab; Nate, Kurt, Brandon, for their support and comradery. Without it, I do not think I would have been able to stay sane on this journey. You never have all the skills required for each journey. Writing is not my skill, thank you Nate and Sal for reviewing multiple times and in quick order, also Sunflower, Wendy and Sarah for also reading through and catching errors.

Friends that distract, help de-stress and continue to encourage are also an important part of this journey. Friends of Global Intervarsity, Clive, Hans and family, Gemechis, Max, Ying, Qiang, John, Laura and Anjana. Also, the Alpha Phi Omega brothers that understand servicing others make the world a better place, and long-time army buddy, motivator and encourager Wendy.

Abstract

This work proposes and shows that thermomagnetic convection could be used in zero gravity to cool components of a Hall-effect thruster. A ferrofluid cavity was develop in the thermal and geometric model of a Hall-effect thruster. Simulations show that with an Ionic Liquid Ferrofluid after two minutes of thruster operations thermomagnetic convection occurs and in zero gravity will produce a larger velocity then natural convection that occurs in earth gravity. However, experiments did not result in heat transfer enhancement due to the limitation of the ferrofluid. Replacement of the Ferrotec EFH1 dispersant with dodecylbenzene did not result in Ionic Liquid Ferrofluid equivalent ferrofluid and did not lower of vapor pressure as intended and limited test to 60 °C. This limitation did not allow for the fluid to experience the largest difference in magnetic susceptibility that occurs near the Curie temperature.

1 Introduction

1.1 Motivation

Ferrofluids were originally created in 1965 by Solomon S. Papell while working with NASA on a solution to migrate fuel towards the outlet of a rocket in zero gravity [1]. Since their invention, ferrofluids have been used in several other areas including being used to cool and improve the sound quality of speakers [2], create targetable medication [3], cool computer chips [4], and separate materials in heterogeneous mixtures [5].

The first U.S. built Hall-effect Thruster (HET) was used on the Air Force Research Lab's TacSat- 2 satellite in December of 2006. More recently, a Hall-effect thruster was used to salvage the mission of the Air Force Advanced Extremely High Frequency (AEHF) satellite after the main thruster failed in 2012 [6, 7].

Overheating of the magnetic circuit is one design challenge for an HET. This work proposes using ferrofluids for cooling the HET's magnetic circuits. Currently, Hall-effect thrusters are cooled by conduction in the body of the thruster through the satellite body and radiated to space. Several studies have attempted to cool an HET by adding large pieces of copper or creating fins to increase surface area. This researcher has not found any articles on cooling HETs using other methods to include heat pipes or electrohydrodynamic cooling [8, 9] . This method adds weight and requires more real estate for the thruster, which requires more fuel and increases cost.

Typically, an HET is cylindrically shaped (Figure 1.1a). Electromagnets are arranged externally around the thruster on the base plate of the thruster, with the main thruster body at the center forming part of the magnetic circuit (Figure 1.1b). The other half of the magnetic circuit runs through the base plate, the bottom of the thruster, the inner core, and a top plate connecting back to the top of the external electromagnets. The gap created by the outer wall and inner core creates an annular channel. A cathode attached to the thruster releases electrons that are than trapped in the magnetic field created across of the gap of the annular channel. These electrons collide with propellant, typically an inert

gas like xenon, released near the bottom of the channel. This interaction of gas and electrons creates ions that are ejected out of the channel due to the electric field creating thrust and heat.

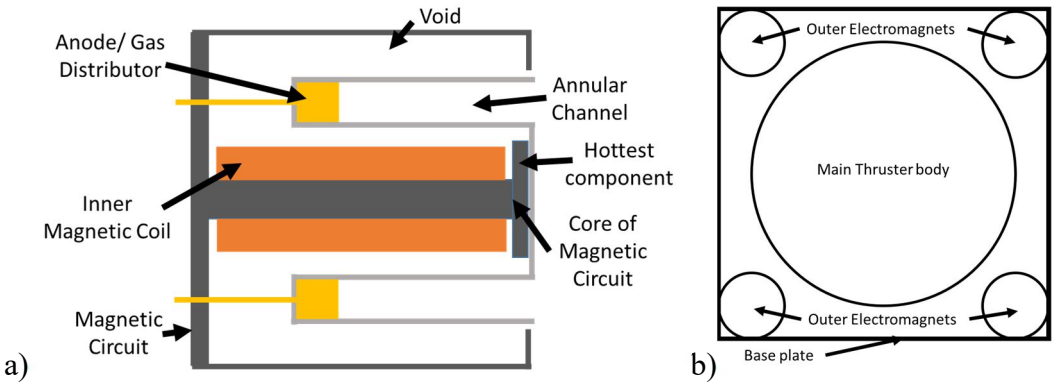

Figure 1-1 a) Schematic of a cross section of a typical radially symmetric Hall-effect thruster. b) Top view of Hall-effect thruster

The body of the thruster makes up the magnetic circuit, so keeping it cool and under the Curie temperature is critical to the thruster operations. The heat produced by thruster operation causes a decrease in magnetization of the magnet circuit. Research and development of HETs has shown that the top of the inner core is the hottest part of the thruster, becoming the most critical part to cool due to the fact that it is part of the magnetic circuit [10].

Ferrofluids are used in heat transfer application because the nanoparticles in the presence of a magnetic field can enhance the heat transfer capability of the fluid. Ferrofluids are a type of nanofluid. Nanofluids contain nanoparticles coated in a surfactant. These coated particles are placed in a carrier fluid called the dispersant. Ferrofluids contain ferromagnetic nanoparticles. The surfactant coating on these ferromagnetic particles allows the fluid to behave magnetically. The particles do not clump like typical iron filings would in the presences of a magnetic field. The particles maintain a distance as large as the surfactant coating, allowing the particles to maintain a fluid motion under the presence of a magnetic field.

Natural convection occurs because the temperature gradient in the fluid creates a density difference in the liquid. Warm fluid is less dense then cold fluid, typically gravity causes the less dense (warm) fluid to migrate up while the denser (cold) fluid settles resulting in the convective flow. This convective flow enhances heat transfer more than simple conduction. This convective motion does not occur in simple conduction.

Natural convection requires gravity to occur. Thermomagnetic convection is a form of convection that occurs in ferrofluids due to the present of a magnetic field and the difference in magnetic susceptibility created by a temperature gradient. Meaning thermomagnetic convection would occur in microgravity because it does not depend on gravity to occur.

Consider a reservoir of ferrofluid. At the left wall of the reservoir there exists a high magnetic field, and on the right wall there is a low magnetic field. The left wall is held at high temperature, and the right wall is held at a cold temperature. The ferrofluid along the hot wall has a lower magnetic susceptibility than the fluid along the cold wall. These cooler particles move in towards the high magnetic field, pushing out the heated particles, creating a convective cell. This process is called thermomagnetic convection. Thermomagnetic convection will have the greatest effect when there is a temperature gradient such that the high temperature is located near a high magnetic field and the low temperature is located near a low magnetic field.

A HET has a U-shaped void within the annular channel that could be filled by a ferrofluid cavity (Figure 1-1). The cavity would experience a high magnetic field where the maximum temperature would also occur. This happens near the top of the annular channel, near the top of the inner core (center of the thruster). The cavity would also have a region of lower magnetic field and lower temperature, located near the bottom of the thruster. This temperature difference and magnetic field create conditions that lead to thermomagnetic convection.

Ferrofluids come in many different types. The nanoparticles used in a ferrofluid can be chosen to fit a specific application. Typical applications, but not generally cooling

applications, have been using Fe_2O_3 nanoparticles which are easily produced. Researchers using ferrofluids in cooling applications have found that modifying Fe_2O_3 to increase the Curie temperature yielding temperature sensitive ferrofluids. Temperature sensitive ferrofluids are fluid with a nanoparticle curie temperature below the decomposition or boiling temperature of the fluid. Recently, researcher at the University of Sydney created a stable ferrofluid of Fe_2O_3 nanoparticles with an ionic liquid [11]. This ferrofluid was able to withstand higher temperature due to the decomposition temperature of the ionic liquid being higher than typical fluids used for ferrofluids. This ferrofluid can now withstand high temperatures with simply made Fe_2O_3 nanoparticles. This ferrofluid is ideal for the proposed application.

This work proposes an application would not need additional space because it would fill a void that already exists in the thruster design. This free convective setup would not require any additional pumps that a forced convective set up would. There is also no power requirement because this application would use the existing magnetic field. The only additional weight is that of the fluid and the container that holds it. Interestingly, the weight of Ionic Liquid Ferrofluid (ILFF) needed (~63.4 g) would be less than 3% of a single ¼ inch copper plate double the size of the back of the thruster used as to radiate heat (~1845 g).

1.2 Literature Review

There is a large body of research on ferrofluids for heat transfer applications, however few for applications for microgravity environments and cooling Hall-effect thrusters. Recent research may reveal if the conditions within the proposed cavity are ideal for thermomagnetic convection. Research will also show what conditions will be optimal for heat transfer enhancement.

1.2.1 Strength of the Magnetic Field and Temperature Difference

Numerical and experimental studies have shown the effect of both large and small magnetic fields and temperature differences [12-14]. Hadavand analytically showed that

thermomagnetic convection will dominate over natural convection in a convective cell [12]. His set up included a square cavity with 2 mm long walls, with the top and the bottom wall adiabatic, the left and right wall were held at a constant temperature. The left wall was held at a warmer temperature than the right wall. An electromagnet created a dipole moment in the middle of the bottom wall below the cavity, which created a non-uniform magnetic field. He varied the magnetic field strength from 0 to .2 A/m (0-.002 Gauss). He also varied the temperature difference from 15-90 K. He found that in the presence of gravity, for large temperature differences and large magnetic fields, the average Nusselt number was also large [12]. Large Nusselt number means that convection dominated heat transfer.

Ashouri showed that thermomagnetic convection will dominate in the convective cell using a semi-implicit finite volume numerical method for a free convective case [13]. His setup was like Hadavand's setup; Ashouri had a square cavity with top and bottom walls adiabatic, the left wall held at a constant temperature. The right wall was the cold wall, but it was not held at any constant temperature. Ashouri also had a permanent magnet placed symmetrically under the bottom wall producing a non-uniform magnetic field within the cavity. Ashouri found that in zero-gravity conditions the magnetic field must be larger than a threshold value to create a thermomagnetic convective cell. The magnitude of the threshold magnetic field is dependent on many factors including the composition of the nanoparticles, the viscosity of the ferrofluid, and volume fraction of the nanoparticles[13].

Krauzina conducted an experiment demonstrating a free convective case, in a thermally isolated sphere, in order to isolate the magnetic effect [14]. A heat exchanger was placed on the top and bottom of the sphere. This setup was also sandwiched by an electromagnet on the top and bottom. Using a uniform magnetic field and heating from the bottom, they proved that thermomagnetic convection and natural convection cancel each other and inhibit heat transfer. With no magnetic field and heated from the top, the ferrofluid increased heat transfer by 10% compared to the carrier fluid without nanoparticles. In the presences of a large magnetic field, the ferrofluid increased heat transfer by a factor of two.

Both numerical studies and Krauzina's experimental study show that for a large enough magnetic field and temperature difference, thermomagnetic convection will dominate in the convective cell. These conditions exist in an HET. In an HET, the magnetic field strength near the top of the gap of the annular channel is normally larger than 8000 A/m (100 Gauss). The field within the proposed cavity would be non-uniform with the largest magnetic field occurring near the top of the annular channel. The proposed ferrofluid cavity is like the setup used by Tomaszewski. He achieved a temperature difference of 298 K in a 200W thruster between the thruster body near the exit of the annular channel and the bottom of the thruster body [10, 15].

1.2.2 Shape of the Cavity

The shape of the cavity is not fixed, but it is limited by the thruster design. Optimal cavity shapes are those that enhance heat transfer more for the given application. Multiple optimal cavity shapes have been explored by Banerjee, Mojumber and Kruazina for non-HET cooling applications [16-19].

In a free convective case, Banerjee numerically showed that the shape of the cavity had an influence on the shape and size of the thermomagnetic convective cell and location of heat dissipation [16]. Banerjee tested a square cavity and a rectangle cavity. In Banerjee's setup, he placed a line dipole near the bottom of the cavity creating a non-uniform magnetic field. Both the top and the bottom walls were adiabatic while the left and right walls were cold walls. Two heaters were place symmetrically on the bottom wall. The square cavity created a convective cell such that the heat was dissipated through the heat sink, as expected. However, in the rectangular cavity, the heat dissipated through the wall near the heat source, which was an unwanted result when trying to cool the heat source. This demonstrates the importance of cavity shape.

In a free convective case, Mojumder numerically studied a semi-circle cavity using finite element analysis [17]. He placed two half-moon shaped heaters on the flat bottom surface of the semi-circle cavity (Figure 1-2). After studying heat transfer of different shapes, Mojumder chose two half-moon shaped heaters because it showed the greatest heat

transfer enhancement. The bottom surface was adiabatic, the round upper surface was held at a substantially lower temperature then the heaters. In this study, he varied the angle of the magnetic field on the cavity. Under the influence of gravity, he found the optimal angle (θ) for the magnetic field for heat transfer enhancement was 45° (Figure 1-2).

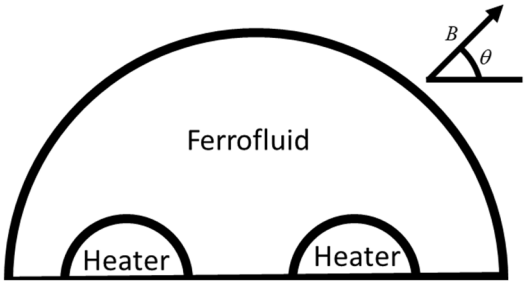

Figure 1-2 Shape of Mojumder Cavity

Additionally, Mojumder studied a C-shaped cavity using a cobalt-kerosene ferrofluid [18]. The C-shaped cavity was created out of a square with a notch cut out of the right wall (Figure 1-3). The top and bottom wall and the remaining portion of the right wall were adiabatic. The left wall was held at a high temperature and the notch was held at a low temperature. For a ferrofluid with 15% volume fraction, Mojumder found that the ferrofluid enhanced heat transfer more than just the dispersant and natural convection.

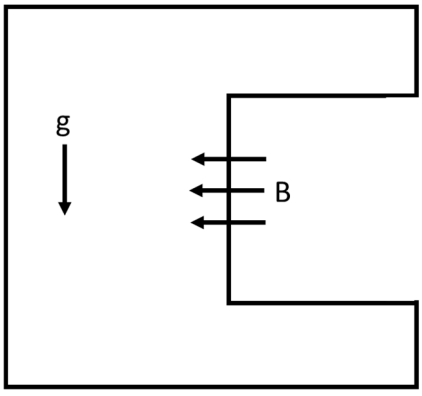

Figure 1-3 C-shaped cavity of Mojumder study

Kruazina, experiment described in 1.2.1, and Bozhko studied the effect of the magnetic field on a fluid in a spherical cavity [14, 19]. They concluded that the location of

the heat source had a noticeable enhancement in heat transfer. The above discussed literature has diversity in cavity shapes with comparable success in heat transfer enhancement. The shape of the proposed ferrofluid cavity and the conditions in a HET for magnetic field and heat source were not specifically studied by other researchers, although the conditions used here are comparable. A numerical study of the proposed cavity will be covered in chapter two to explore what cavity shape will create conditions for thermomagnetic convection to occur.

1.2.3 Position of the Magnetic Field

The magnetic field's orientation is fixed and cannot be changed without modifying the thruster's operation and design. Research done for other applications shows enhancement in heat transfer for different locations of heat sources and magnetic field source. In a forced convective case, Li and Xuan experimentally tested the orientation of the magnetic field. Ferrofluid flowed through a rectangular pipe [20]. In the pipe was a fine tungsten wire that was heated and perpendicular to the flow of the fluid. They concluded that in a uniform magnetic field there is little enhancement to heat transfer compared with natural convection. If the magnetic field is in line with the flow, heat transfer is significantly increased which validated Mohammad's mathematical model [21].

Sheikhnejad studied a 1-meter long section of horizontal pipe [22]. He wrapped the pipe with a heater rope to produce a constant heat flux. The fluid flowed past a non-uniform magnetic field perpendicular to the pipe. Thermocouples were then placed every 10 cm after the magnet. He also added a piece of porous material and noted that the combined method increased the heat transfer by a factor of 2.4. He noted that a different placement of the magnet along the pipe could further enhance heat transfer.

Li and Sheikhnejad's studies show that the fluid flows in-line with the magnetic field. For the proposed application in a HET, this means that flow will initially be in line with the magnetic field across the top of the cavity before hitting the wall of the cavity.

Yang used COMSOL simulations to model simple thermomagnetic convection in a beaker [23]. Yang placed a beaker of ferrofluid on a heat sink and placed a heat source on the surface of the fluid. She varied the position of the magnet along the height of the beaker creating a non-uniform magnetic field in the fluid. She showed that the optimal position of the magnet was half way between the heat source and the heat sink. Yang also conducted a test with different volumes with the magnet placed near the top of the fluid and found that the optimal aspect ratio for thermomagnetic convection was when the diameter of the beaker and the height of the fluid were similar [23]. She verified these simulations with experiments. Both experimentally and analytically, she proved that thermomagnetic convection would dominate convection in 150 ml and less of ferrofluid.

Although the position of the magnetic field cannot be changed in the proposed cavity, Yang's experiment showed that thermomagnetic convection would still occur when the heat source and the high magnetic field are in the same location. A numerical study of the proposed cavity will be conducted and covered in chapter two to ensure the magnetic field and heat source locations will create conditions for thermomagnetic convection to occur.

1.2.4 Volume Fraction

In a free convective case, Sheikoleslami analytically, using the Lattice Boltzmann method, shows that volume fraction and size of the nanoparticles affect heat transfer capability [24]. In his study, he used a square cavity heated from the bottom with a magnetic source above the square cavity. He found that the Nusselt number decreased with increased volume fraction and increased particle size. Implying that to increase convective heat transfer the size of the particles needs to decrease and the volume fraction of the nanoparticles needs to increase. For the proposed application, the ferrofluid should have small nanoparticles and an increased volume fraction to maximize heat transfer.

In the forced convective case, Sheikhnejad demonstrated that an increase in volume fraction of nanoparticles enhances heat transfer; however, he also found that this decreases

the viscosity of the fluid [22, 25, 26]. In free convection, lower viscosity liquids would require more force to induce thermomagnetic convection, thus requiring higher magnetic fields. In a HET, the magnetic field is at a set strength; however, the volume fraction of the fluid can be adjusted to maximize heat transfer.

1.2.5 Bloch Law Difference

Magnetic saturation of coated nanoparticles has been shown to be different than the bulk material. In a free convective case, D. Ortega studied the size and surfactant coatings of both maghemite and magnetite to find a relationships between the temperature and the magnetization saturation of the bulk particles [27]. He found that the ferrofluid studied did not follow Bloch's law. Bloch's law establishes a relation between magnetization saturation of the bulk particles and the temperature experienced by those particles. The conclusion was that ferrofluids have different Bloch exponents due to the reduced size of the particles. This temperature dependent magnetization would affect magnetization of the fluid. The equations developed by Ortega are used later in this chapter to define temperature dependent magnetization of the ferrofluid.

1.2.6 Temperature Sensitive Ferrofluids

Upadhyay developed a temperature sensitive ferrofluid; he states:

> *In certain applications (e.g. energy conversion devices) it is necessary to use a fluid with a large pyro magnetic coefficient, i.e., with a high saturation magnetization and low Curie temperature. Magnetite particles are unsuitable for this purpose since they have Curie temperature higher than the boiling point of a carrier liquid.*

Upadhyay develops a ferrofluid with a 340K Curie temperature and saturation magnetization of 150 G. Many other studies have developed specific nanoparticles with lower Curie temperature in an effort to enhance heat transfer [28].

1.2.7 Microgravity

Theng Yee Chong shows experimentally in microgravity the direction of the magnetic field influences the motion of the fluid [29]. Theng put a drop of ferrofluid on the north and south poles of a magnet, with the north side on top of the magnet. They performed these tests in an airplane that flew in a parabola to create microgravity for 10-20 seconds. When a droplet or small volume of ferrofluid is placed near a magnetic field, it creates spikes on the fluid surface. These spikes are the nanoparticles aligning with the magnetic field lines of the magnet. Theng showed that more spikes developed on the surface on the North Pole (top side) than the South Pole (bottom side) in micro gravity. This showed that the direction of the magnetic field affects the fluid response in microgravity.

In the proposed application the magnetic field strength has a fixed range that the thruster requires to operate correctly. The direction of the magnetic field and strength of the heat source are set by the thruster design. The response of the ferrofluid is a function of direction and location of the magnetic field, this will inform the design of the proposed application.

In a free convective case, Odenbach experimented in drop towers and sounding rockets [30]. Odenbach created a ferrofluid cavity in between two cylinders (Figure 1-4). The inner cylinder was heated, and the outer cylinder was held at constant temperature by a latent heat reservoir. He created an azimuthal magnetic field, which in turn created a radial magnetic field gradient. Zero gravity test are limited to 10-20 secs. Odenbach showed that the results from 10-20 secs was enough to prove that thermomagnetic convection current was established but not long enough to comment on heat transfer enhancement.

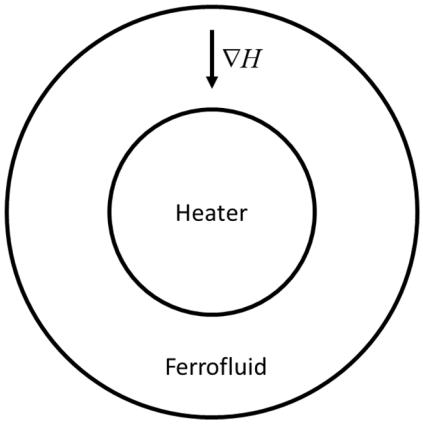

Figure 1-4 Odenbach Experimental Cavity

Drop towers, sounding rockets, and planes have been used in an attempt to prove these theories in microgravity and all three approaches state that 20-30 seconds is enough time to see the onset of thermomagnetic convection [29, 30]. Longer tests are needed to demonstrate the effect on heat transfer. The system needs to attain a steady state to see the heat transfer enhancements, which cannot be achieved in 20-30 seconds. The system would need 20-30 minutes depending on the size of the system.

In Suslov's article, he lays out a plan to conduct ground-based work to prove that certain applications will work in space [31]. He supports results of experimental work on earth but emphasizes validating them with simulations. The simulations isolate the effects that would occur in microgravity and ignore those caused by gravity. Ultimately, he advocates for experimentation in zero gravity, specifically on the International Space Station to observe the isolated effect of the magnet field on the ferrofluid and to test application that ferrofluids are well suited for heat transfer application in space.

This work on cooling on a HET will include a numerical study conducted in COMSOL Multiphysics and an experimental study using a thermal model of a HET (Chapter 2). According to Odenbach, further research could be conducted in microgravity by using sounding rockets and drops towers.

1.3 Thermomagnetic convection

1.3.1 Magnetization of the fluid and volume force equation

The magnetic field exerts a force on the fluid, specifically the nanoparticles, which cause it to react to magnetic fields as described above. This body force is what causes thermomagnetic convection. Rosensweig states that the body force is equal to [32]

$$\mathrm{f_{body}} = -\nabla[\mu_0 \int_0^{\mathbf{H}} [\mathbf{v}\left(\frac{d\mathrm{M}}{d\mathrm{v}}\right) d\mathrm{H}] + \mu_0 \int_0^{\mathrm{H}} \mathrm{MdH}] + \mu_0 \mathrm{M}\nabla\mathrm{H} \tag{1.1}$$

where μ_0 is the permeability of free space, M is the magnetization, H is the magnetic field strength, and v is volume.

Because we are concerned with a liquid that is largely incompressible, we can drop the first term and the body force becomes:

$$f_m = \mu_0 \left(-\nabla \int_0^H MdH + M\nabla H \right). \tag{1.2}$$

We can expand the integral term:

$$\nabla \int_0^H MdH = M\nabla H + \int_0^H \nabla M dH\,, \tag{1.3}$$

$$\nabla \mathbf{M} = \frac{\delta M(T,H)}{\delta x} = \frac{\delta M(T,H)}{\delta T}\frac{\delta T}{\delta x} = \frac{\delta M(T,H)}{\delta T}\nabla T\,, \tag{1.4}$$

where T is the temperature. When equation 1.4 is put into equation 1.3 we obtain

$$\nabla \int_0^H MdH = M\nabla H + \int_0^H \frac{\partial M}{\partial T}\nabla T dH \tag{1.5}$$

The magnetization also can be represented by the magnetic susceptibility

$$M(T,H) = \chi(T,H)H\,, \tag{1.6}$$

where χ is the magnetic susceptibility. With some manipulation

$$\nabla\int_0^H MdH = M\nabla H + \int_0^H \frac{\delta(\chi(T,H)H)}{\delta T}\nabla T dH\,, \tag{1.7}$$

$$= M\nabla H + \int_0^H \nabla T H \frac{\delta\chi(T,H)}{\delta T} dH\,, \tag{1.8}$$

$$= M\nabla H + \nabla T\int_0^H \frac{\delta\chi(T,H)}{\delta T} HdH\,. \tag{1.9}$$

If we insert this back into body force equation, we obtain:

$$f_m = -\mu_0[M\nabla H + \nabla T\int_0^H \frac{\delta\chi(T,H)}{\delta T} HdH] + \mu_0 M\nabla H \tag{1.10}$$

The $\mu_0 M\nabla H$ terms cancels out and the body force term becomes:

$$f_m = -\mu_0\nabla T\int_0^H \frac{\delta\chi(T,H)}{\delta T} HdH \tag{1.11}$$

Equation **Error! Reference source not found.**(1.11) shows that the body force is a function of the strength of the magnetic field (H), the temperature gradient (∇T), and the magnetic susceptibility is a function of both temperature and the magnetic field ($\chi(T,H)$). This equation also shows that the direction of force is along the thermal gradient.

We need to establish an equation for magnetic susceptibility as a function of temperature and H ($\chi(T,H)$). Equation (1.6) shows that ($\chi(T,H)$) is a function of magnetization (M) and (H). Rosensweig defines the magnetization of a ferrofluid by the Langevin function:

$$M(T,H) = (\coth(\alpha) - \frac{1}{\alpha})\phi M_d \tag{1.12}$$

$$\alpha = (\frac{\mu_o M_d H d^3}{\kappa T}) = \frac{mH}{kT} \tag{1.13}$$

where ϕ is the proportion of nanoparticles by volume and M_d is the saturations magnetization of the bulk particles, k is the Boltzmann constant and μ_0 is the permeability of free space [6]. Alpha represent the energy ratio mH/kT. The magnitude of the magnetic moment(m) multiplied by the applied field (H) is the magnetic potential energy. Boltzmann constant (k) multiplied by the temperature (T) is the kinetic thermal energy.

1.3.2 Magnetization of nanoparticles as function of temperature

The only unknown in equation (1.12) is M_d, the saturation magnetization of the bulk magnetic particles. Until recently M_d was a chosen as to replicate the bulk magnetic saturation of the chosen ferromagnetic material or it was held constant because of small temperature difference in the application for cooling. However, magnetic saturation of ferromagnetic materials changes with temperature. Magnetic saturation of the bulk magnetic particles (M_d) is thus temperature dependent and also varies depending on the surfactant coating.

As explained previously, Ortega expands on a relationship between the saturation magnetization and temperature of the nanoparticles within a ferrofluid [27]. The relationship that described the magnetic saturations of nanoparticles in a fluid is Bloch's Law, which states:

$$M_d(T) = M_d(0)(1-(\frac{T}{T_c})^{3/2}) \tag{1.14}$$

Ortega proves Bloch's law needs to be modified, after several experiments in the temperature range of 25 K to 350 K, as follows for oleic acid-coated Fe_2O_3 nanoparticles:

$$M_d(T) = 31.72(1-2.59e^{-6}T^2) \tag{1.15}$$

The magnetic saturation of the bulk magnetic nanoparticles decreases with the increase in temperature (Figure 1.5). As the temperature rises the saturation magnetization decreases. If the magnetization of entire fluid is not homogenous, thermomagnetic convection can occur. If there is a difference in magnetic susceptibility within the fluid thermomagnetic convection can occur. However, it will only enhance heat transfer when the difference in magnetic susceptibility is large enough to produce a heat transfer rate higher than conduction in zero-gravity and natural convection in earth gravity. It will also enhance heat transfer is there is a decrease maximum temperature as compared to conduction in zero-gravity and natural convection in earth gravity. This difference in magnetization creates movement in the fluid without gravity. The body force on the fluid with Fe_2O_3 nanoparticles can now be fully defined by equations (1.11), (1.12), (1.13), and (1.15).

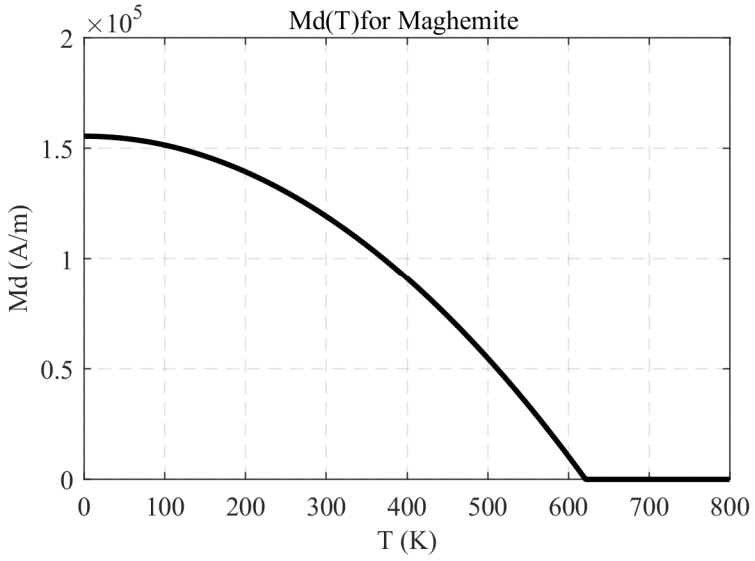

Figure 1-5 Magnetic saturation of bulk magnetic particles (Md(T)) vs temperature

1.3.3 Magnetic properties of the fluid

Magnetic saturation of the fluid decreases with increased temperature (Figure 1-6). Figure 1-6 shows the magnetization of the ferrofluid versus magnetic field at various temperature. The fluids' magnetization plot is similar to other magnetic materials, further

showing that the liquid has magnetic behaviors. The figure also shows that saturations occurs around $3x10^5$A/m. The maximum magnetic field strength in the proposed ferrofluid cavity is around $5.5x10^4$A/m.

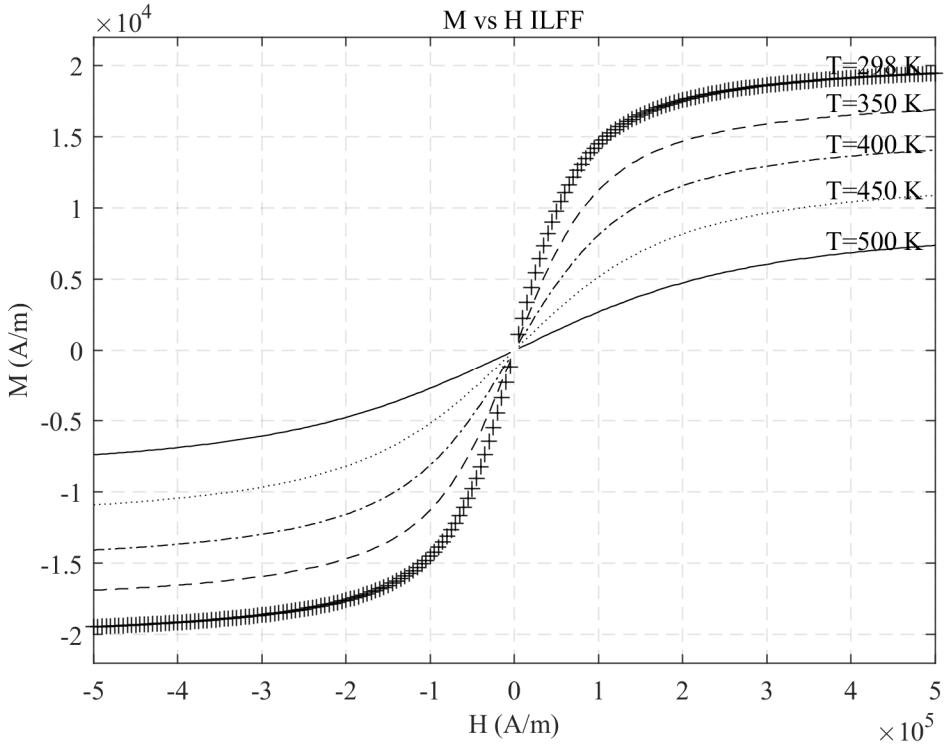

Figure 1-6 Magnetization versus the magnetic field strength

As the magnetic field strength increases, the magnetic susceptibility decreases (Figure 1-7). As the magnetic field strength increases and reaches magnetic saturation, there is a quicker decline in magnetic susceptibility. As seen from the studies above, large temperature differences enhanced heat transfer more than smaller temperature differences. The large temperature difference leads to larger differences in magnetic susceptibility (Figure 1.7). As temperature increases, the magnetic susceptibility decreases. Near the Curie temperature the magnetic susceptibility drops more quickly. Strong convective flow will occur when the temperature is near the curie temperature, because of this sharp difference in magnetic susceptibility. The temperature range of a system should encompass this temperature range so that thermomagnetic convection can be optimized.

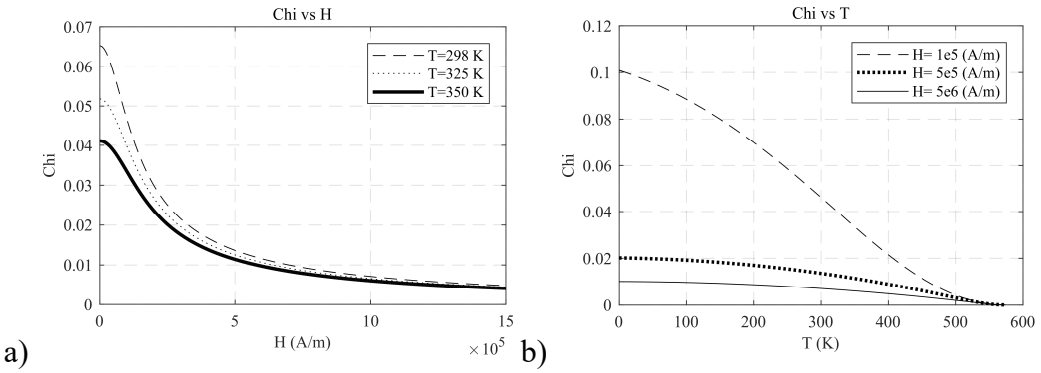

Figure 1-7 a) Magnetic susceptibility (Chi) vs magnetic field (A/m) strength for ILFF b) Magnetic susceptibility vs temperature (K) for ILFF

These two effects combined lead to thermomagnetic convection. Increasing the magnetic field to around the saturation magnetization and increasing the temperature difference will lead to a greater thermomagnetic convective cell. However, the temperature range of the gradient should encompass the Curie temperature of the nanoparticles and be large enough to see a significant change in magnetic susceptibility (Figure 1-8).

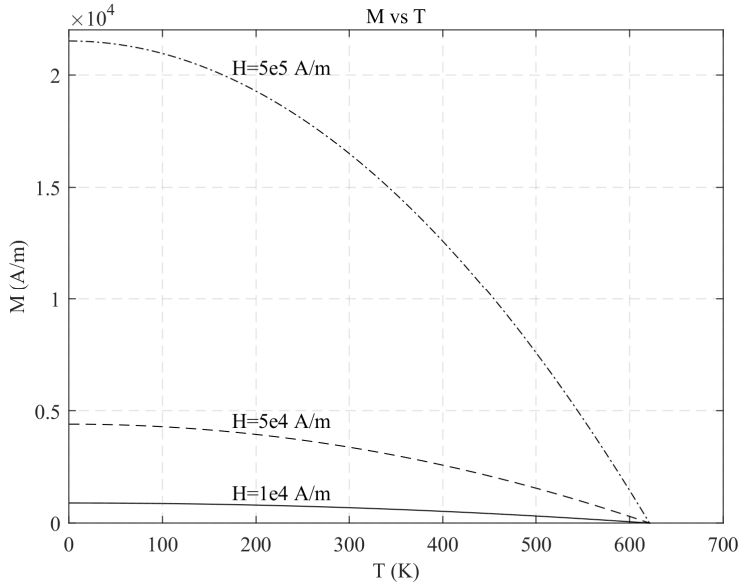

Figure 1-8 Magnetization of the Ferrofluid versus the temperature at various magnetic field strength

In the proposed ferrofluid cavity, the magnetic field strength is set by the design of the HET. The material of the nanoparticles in the fluid could be chosen so that the magnetic saturation is equal to or slightly above the magnetic field strength of the HET in order to create conditions for maximum difference in magnetic susceptibility. This would allow the system to see strong convective cells because of the sharp change in magnetic susceptibility that occurs near the Curie temperature. The ferrofluid should also be designed so that the curie temperature of the fluid is near the maximum temperatures of the system is so take advantage of the sharp drop in magnetic susceptibility

1.3.4 Other magnet dependent properties of ferrofluid

The fluid is defined by other physical properties of the fluid; viscosity and thermal conductivity are also influenced by the magnetic field. The viscosity of the fluid will increase the force needed to induce thermomagnetic convection. Seval Genc defines dynamic viscosity of a ferrofluid by

$$\eta_{ff} = \frac{\eta_f}{\left(\frac{3}{2}\right)\phi \frac{\left(\frac{1}{2}\right)\alpha L(\alpha)}{1+\left(\frac{1}{2}\right)\alpha L(\alpha)} + 1} \tag{1.16}$$

η_{ff} =dynamic viscosity of the ferrofluid, η_f = dynamic viscosity of the dispersant, α is equal to the equation above, Equation (1.13) [33].

Seval Genc uses effective medium theory to come up with an equation for the thermal conductivity of a ferrofluid [33]. This equation is a function of volume fraction and properties of both fluid and nanoparticles.

$$\kappa = \left(\frac{1+2\beta\phi}{1-\beta\phi}\right)\kappa_f \tag{1.17}$$

$$\beta = \frac{\kappa_p - \kappa_f}{\kappa_p + 2\kappa_f} \tag{1.18}$$

κ_p = thermal conductivity of the nanoparticles and κ_f = thermal conductivity of the dispersant, while κ is the thermal conductivity of the ferrofluid.

The density of the ferrofluid is calculated with temperature dependent density equation:

$$\rho_{ff}(T) = \frac{\rho_f(T_0)}{\left(\left((T - T_0) * \alpha_F\right) + 1\right)} \tag{1.19}$$

ρ_f is the density of the liquid, α_{ff} is the thermal expansion coefficient, T_0 is the reference temperature.

2 Numerical Simulations

2.1 Simulations Setup

COMSOL Multiphysics was used to conduct the numerical simulations of the test thruster. A 2-D axisymmetric model was created for the following simulations (Figure 2-1). The volume force equation (1.11)**Error! Reference source not found.** was a volume force in the laminar flow module. This along with magnetic susceptibility (Equation (1.6)) defined the motion of the particles in the fluid. The coils were multi-turn coils in the magnetic field module. The electromagnetic heat source module coupled the magnetic field and the heat transfer modules to compute the heat produced by the coils. Maxwell's equations defined the magnetic field and the magnetic interactions between the fluid and the magnetic field in the magnetic fields module. The non-isothermal module coupled the heat and laminar flow of the ferrofluid using Naiver-Stokes equations.

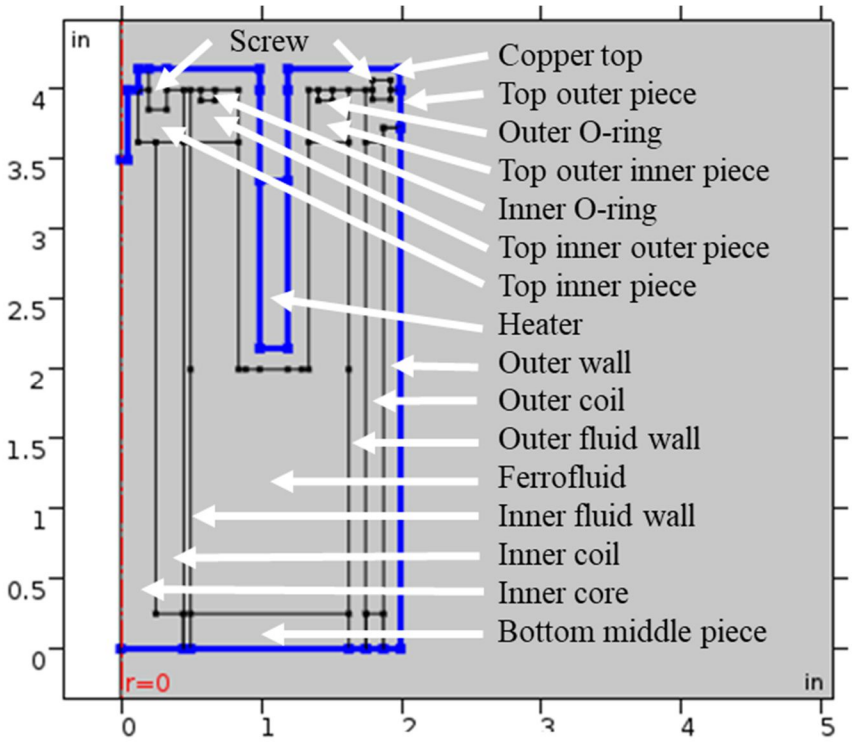

Figure 2-1 2D axis symmetric view of simulation setup

The heat within the annular channel was modeled as a heat source (Figure 2-1). All surfaces that were not in contact with another part of the thruster (outer surfaces) were radiative surfaces with emissivity of .01 for copper surfaces and .31 for steel surfaces (Figure 2-1). The initial temperature of both the thruster and the vacuum was room temperature. The copper channel and the two coils are copper, the inner seal is Kalrez and the outer seal is Viton, the ferrofluid was given physical properties specific to the chosen ferrofluid, all other pieces are steel. The flow within the cavity is laminar flow. Several studies define the motion of the fluid in a free convective cavity or enclosure as laminar flow [34]. The fluid was incompressible as stated previously in chapter one. Figure 2-2 shows the magnetic field lines and field strength throughout the thruster.

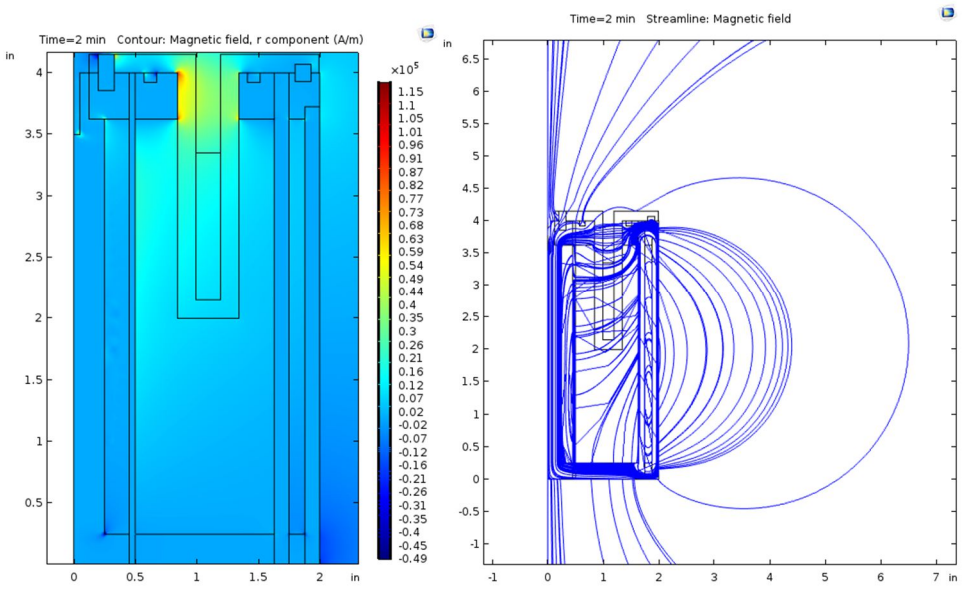

Figure 2-2 a) Magnetic field strength plot (A/m) b) magnetic field line plot with 15A inner coil and 10 A outer coil power setting

To validate the equation derived in chapter one, the simplified setup used by Yang was recreated and simulated with the previously derived equations (Equations (1.2) and (1.15)) [23]. The magnet in this set up was placed at the top on the side of the fluid reservoir. Yang's experimental results discussed in chapter one, were compared to the simulation and showed around a 27 Kelvin temperature difference for the 5 cm high fluid

and 22 Kelvin temperature difference for the 10 cm high fluid (Table 2-1). This showed that the equations derived could model thermomagnetic convection.

Table 2-1 Comparison of Yang experimental results and simulations

Ferrofluid height (cm)	Yang Experimental Steady state temperature (K)*	Simulations Steady state temperature (K)
5	~410	383
10	~455	433

*date from a graph in Yang paper

Typical operating temperatures for a 200W HET are about 770K (496ºC/1418ºF) near the top of the inner core [10]. This temperature is maintained for prolonged periods. The problem with this high temperature is the temperature at which the ferrofluid will decompose. If the system temperature is above the decomposition (break-down) temperature of the chosen ferrofluid, then the fluid will decompose and not produce thermomagnetic convection.

As stated above in chapter one, researchers are currently making low Curie temperature nanoparticles in lieu of finding a fluid that can handle high temperatures. They are doing this so that they can maximize the large difference in magnetic susceptibility near the Curie temperature. Most dispersants decompose at temperatures much lower than the Curie temperature of simple iron-based nanoparticles. Fluids decompose at temperatures that cause the bounds between the individual elements to break and fluid to decompose into those elements.

The Curie temperature of maghemite Fe_2O_3 is around 645 ºC [35]. If these easy produced nanoparticles are used for proposed application, the fluid would need a decomposition temperature higher than 645 ºC. Ionic Liquid Ferrofluid (ILFF) have decomposition temperatures around this range. ILFFs have also been proven to produce stable ferrofluids [11].

The ferrofluid used for these simulations was EMIM-NTF2 ionic liquid[11]. Ionic liquids break down at much higher temperatures. EMIM-NTF2 decomposition temperature is 728K (455ºC/851ºF). The Curie temperature of maghemite Fe_2O_3 is around 645ºC[35]. The maximum temperature of the system (770K) exceeds the Curie temperature of the fluid, allowing for the fluid to be in a temperature region that experiences a large drop in magnetic susceptibility near the Curie temperature [10]. The maximum system temperature is only slightly above the decomposition temperature of the ionic liquid. In COMSOL the ferrofluid was defined by its material properties (Table 2-2).

Table 2-2 Material Properties of ILFF

Property	**Equation**	**Units**
Dynamic Viscosity	Equation **Error! Reference source not found.** (1.16)	Pa*s
Ratio of specific heats	1	1
Density	Equation (1.19)	kg/m^3
Thermal Conductivity	Equation (1.17) and (1.18)	W/(m*K)
Relative permeability	Equation (1.6) **Error! Reference source not found.**	1

The mesh used for the following simulations was user defined. The mesh for the fluid region was made finer then the surrounding sturcture. This fluid region mesh included boundary layers and was configured for fluid dynamics. The mesh for the magnetic curcuit was refined around the sharpe edges. The mimimum quality of the mesh as .2238 and the average quality was .8837, overall the mesh had 103,065 elements.

Simulations in a gravity environment with the magnetic field off show pure natural convection. Simulations in a gravity environment with the magnetic field on show the combination of both nautral and thermomagnetic convection. Simulations in a zero gravity environment and the magnetic field on show pure thermomagnetic convection and

simulations in zero gravity environment with the magnetic field off show pure conduction (Table 2-3).

Table 2-3 Simulation scenarios

	Magnets ON	Magnets OFF
Gravity	Combine natural and thermomagnetic convection	Pure natural convection
Zero-Gravity	Pure thermomagnetic convection	Pure conduction

Simulations with the magnets on and off in a zero gravity environment were compared to see if thermomagnetic convection would be more effective in space than pure conduction. Comparing natural convection in earth gravity with the magnet off to thermomagnetic convection in zero-gravity with magnet on shows which will have larger velocities during convection. If in combination with a larger velocity, the maximum temperature of the system is lowered, we can show that thermomagnetic convection enhances heat transfer with larger velocities. Simulations with the magnets on and off in a gravity environment were compared to see if thermomagnetic convection would enhance heat transfer in ground testing, and to show if thermomagnetic convection could be observed in ground testing. Heat transfer enhancement is a lowering of the maximum temperature in the thruster, specifically near the inner core.

2.2 ILFF Numerical Simulation Results

The simulations below show results after two minutes. Using a Dell Precision T1700 desk top simulations took one to two days to compute to get results for two to three minutes of simulation time. Even with the help of a super computer and multiple processors, up to 16, computation of more than 10 minutes simulation time still took several days.

2.2.1 Zero Gravity with Magnet off vs Magnet on

Zero gravity simulations showed (after two minutes) there is no difference in the maximum temperature of the system, however it does show that when the magnet is on thermomagnetic convection occurs. The heat flows towards the bottom of the thruster with the magnet on and thermomagnetic convection occuring, while heat raditates from the heat source with the magnet off and simple condcution (Figure 2-3). Figure 2-3 shows the temperature range is 300-320 Kelvin with red being the highest temperature and blue the coldest. This shows that in two minutes, thermomagnetic convection is forcing movement in the fluid which moves the heat around the fluid cavity. This movement could reduce the temperature of the system over time.

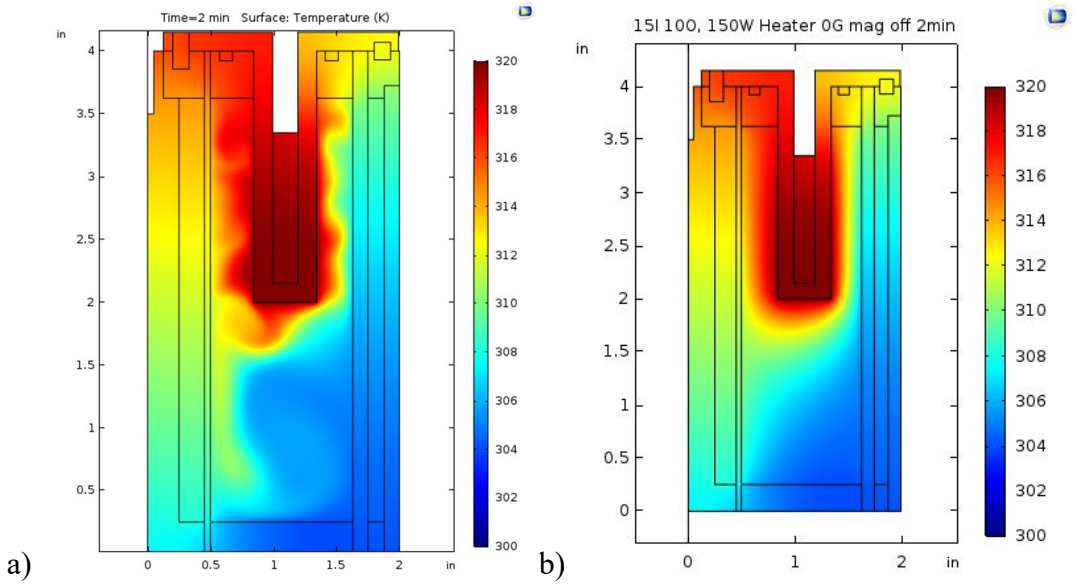

Figure 2-3 Temperature (K) plot of 150W heater with 15 A inner coil, 10 A outer coil in zero gravity with a) magnet on b) magnet off

Zero gravity simulations also showed that the thermomagnetic convection (zero gravity, magnet on) produces motion in the fluid in zero gravity (Figure 2-4). Figure 2-4 shows the velocity throughout the fluid cavity. Larger velocities are red while zero velocity is dark blue. There is fluid movement when the magnet is on because of thermomagnetic convection ocurs, while there is no fluid movement when the magnet is off because there is nothing causing convection. The maximum velocity of thermomagnetic convection in

zero gravity (magnet on) was .05 m/s. Even though the maximum temperature of the system was not lowered, the fluid motion allowed the heat to flow through more fluid, which if allowed to developed over time could decrease the maximum temperature of the system.

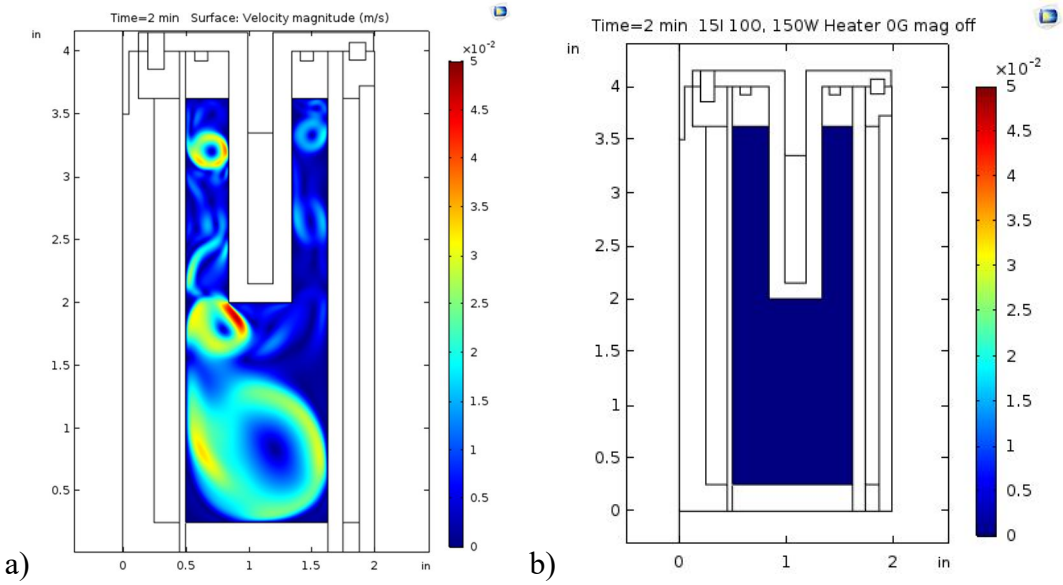

Figure 2-4 Velocity (m/s) plot of 150W heater with 15 A inner coil, 10 A outer coil in zero gravity with a) magnet on b) magnet off

A convective cell is a cycle of cooling that occurs. These convective cells could be any size and have different velocities. Figure 2-4a shows multiple convective cells of different sizes and velocities. There are small convective cells with low velocities in the upper right of the cavity and other small convective cells of the same size with higher velocities in the upper left of the cavity. The figure also shows a large convective cell in the bottom of the cavity. Over time two or more convective cells could merge, specifically the bottom cell and the one cell to the upper left.

2.2.2 Earth Gravity with Magnet off vs Zero Gravity with Magnet on

Comparing simulations with the magnet on in a zero gravity, pure thermomagnetic conduction (Figure 2-5a), with simulations in a gravity enviroment with the magnet off, pure natural convection and conduction (Figure 2-5c) showed that heat was transported

differently. Again there was no differnce in the maximum tempearture of the system or these simulation that are two minutes after w Figure 2-5 shows the temperature in Kelvin throughout the test thruster with red being the highest temperature and blue the coldest. Thermomagnetic convection moved the heat more towards the bottom of the cavity, where natural convection seem to move the heat near the top of the cavity. Natural convection seem to be sinking heat into the heat source, which is an unintended result.

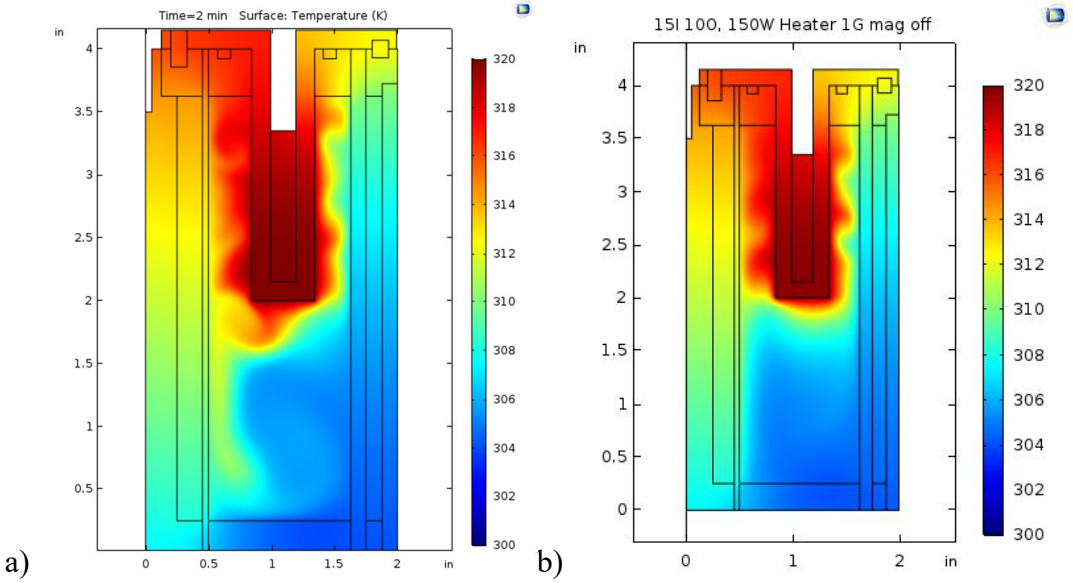

Figure 2-5 Temperature (K) plot of 150W heater with 15 A inner coil, 10 A outer coil in a) zero gravity with magnet on b) gravity with magnet off

The zero gravity enviornment with the magent on simulation (Figure 2-6a) and earth gravity environment with the magnet off simulation (Figure 2-6b) also showed that thermomagnetic convection will produce a greater velocity then natural convection after two minutes of thruster operation. The maximum velocity in earth gravity with the magnet off is .024 m/s and the maximum velocity in zero gravity with the magnet on is .05 m/s.

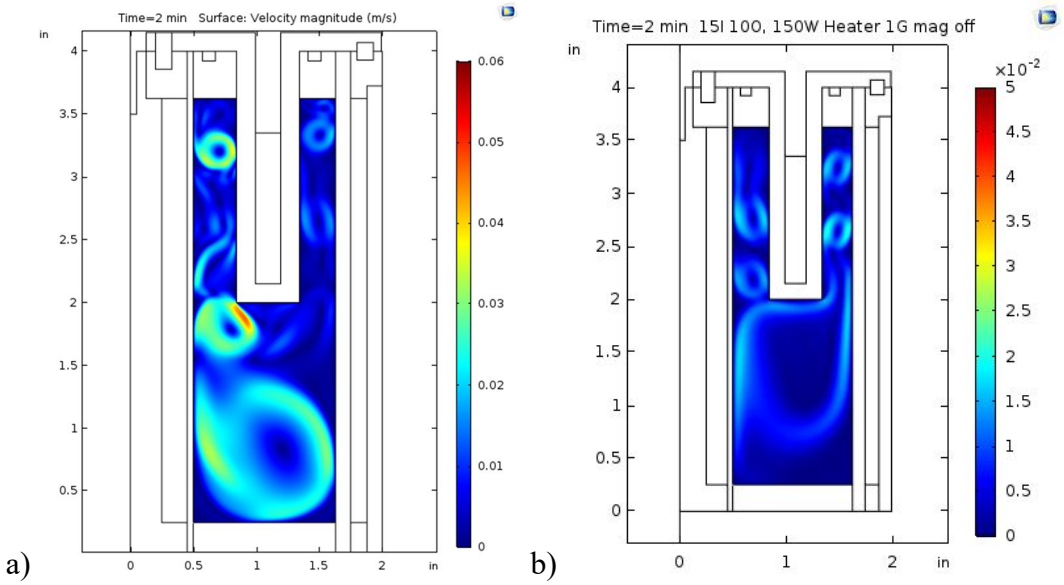

Figure 2-6 Velocity (m/s) plot of 150W heater with 15 A inner coil, 10 A outer coil in a) zero gravity with magnet on b) gravity with magnet off

Figure 2-7 b shows natural convection in earth gravity with the magnet off and the fluid near the top of the cavity in flowing up towards the heat source. Figure 2-7 a shows thermomagnetic convection in zero gravity with the magnet on and that fluid flows generally in a downward direction away from the heat source.

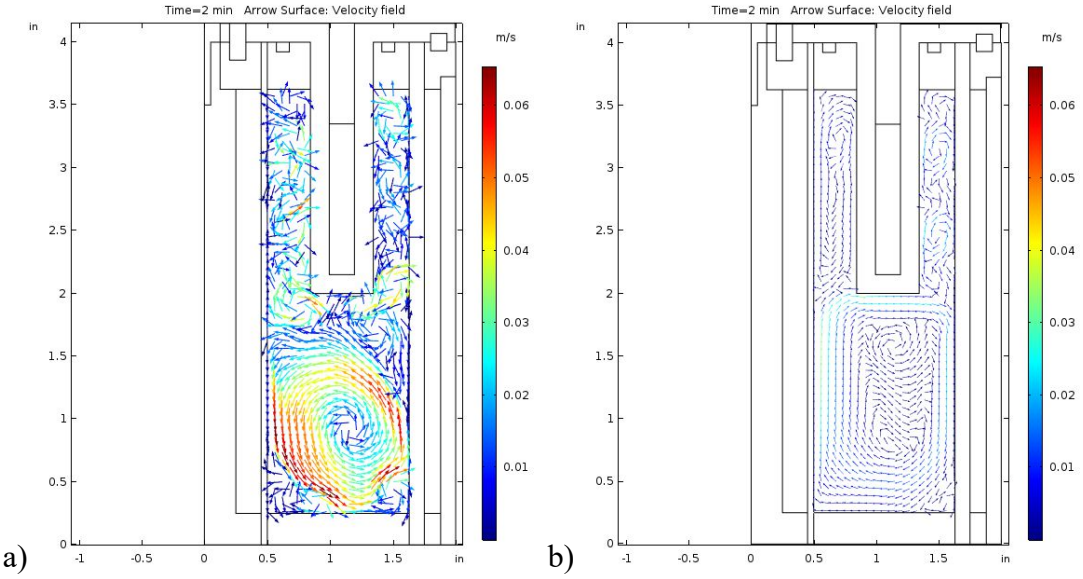

Figure 2-7 Velocity (m/s) arrow plot of 150W heater with 15 A inner coil, 10 A outer coil in a) zero gravity with magnet on b) earth gravity with magnet off

2.2.3 Magnetic field strength in Zero Gravity

Recent studies, discussed in chapter one, have shown that the larger the magnetic field, the larger the heat transfer enhancement. Figure 2-8 shows in zero gravity, with three different magnetic field settings, that the each setting produces motion in the fluid that moves the heat away from the heater and towards the bottom of the fluid cavity. Figure 2-8 shows hot temperatures in red and cooler temperatures in blue; temperature is in Kelvin. The temperature difference between the magnetic field on and off was zero Kelvin for each setting. The power input is increased with an increased magnetic field strength because of the electromagnets. Due to this power increase, the stronger the magnetic field the hotter the overall system will be. This is the reason figure 2-8 a and d have a higher temperature then figure 2-8 c and f. There may not be a large temperature difference between the three different test, but the motion of the fluid is causing the heat to flow towards the cooler regions of the thruster.

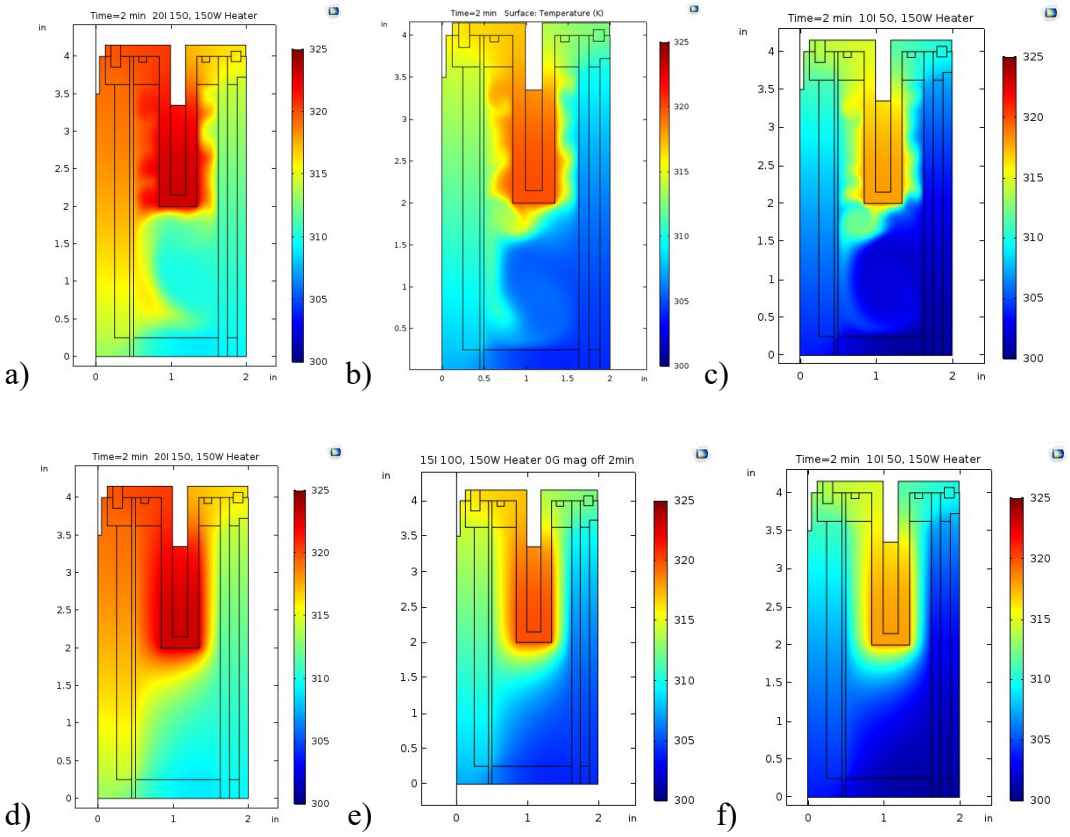

Figure 2-8 Temperature (K) plot of 150W heater in zero gravity with magnet on with a) 20 A inner coil, 15 A outer coil (900 Gauss) b) 15 A inner coil, 10 A outer coil (700 Gauss) c) 10 A inner coil, 5 A outer coil (600 Gauss). With magnet off d) 20 A inner coil, 15 A outer coil e) 15 A inner coil, 10 A outer coil f) 10 A inner coil, 5 A outer coil.

Table 2-4 shows the magnetic field strength and maximum velocity of three different power settings in zero-gravity conditions. The maximum velocity occurred with the lowest magnetic field strength. The reason for this could be that the simulations are only show a snap shot at two minutes. If the simulations where run out for 90 minutes we would see steady state conditions. Simulation took too much time to compute and where only run for two minutes of simulation time. However, this does show that there is motion in the fluid for multiple magnetic field settings.

Table 2-4 Simulation results

Coil settings	Gravity settings	Magnet Setting	Maximum Magnetic Field (W/m^2) Strength (Gauss)	Maximum Velocity (m/s)
20 A inner coil 15 A outer coil	Zero-Gravity	On	900	.0393
15 A inner coil 10 A outer coil	Zero-Gravity	On	700	.05
10 A inner coil 5 A outer coil	Zero-Gravity	On	600	.05938

These simulations show thermomagnetic convection will produce a larger velocity in weaker magnetic fields, but stronger convective cells occur in a stronger magnetic field. The stronger the cell the higher the velocity of the cell. A cell is seen as a circle or almost circle in figure 2-9. If the cell is almost circle or oblong, it may indicated that two cells are merging or fighting against each other. In the upper left hand corner of Figure 2-9c there is one strong fully developed cell near the middle of the cavity indicited by the red circle meaning high velocity. On the top of this cell is a faint yellow circle which is a weak convective cell and lower velocity. In Figure 2-9a there seems to be two merging cells near the bottom of the cavity, while there are three weak cells in both upper the right and left side of the cavity.

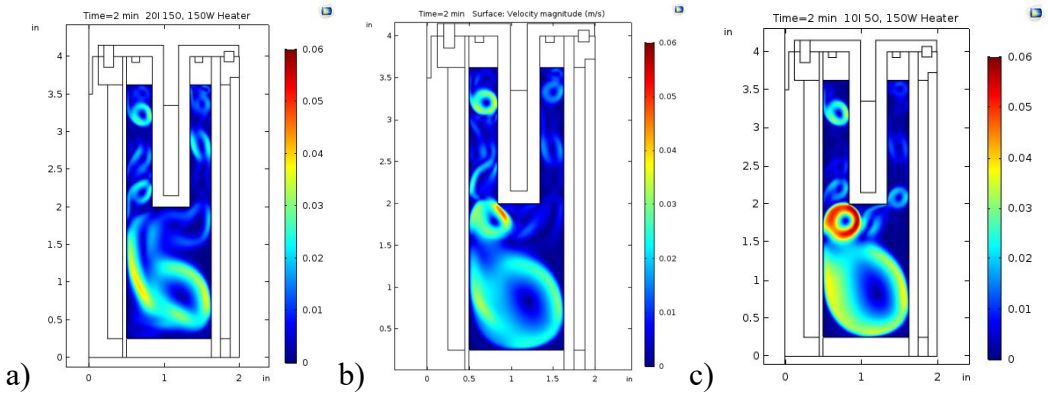

a) b) c)

Figure 2-9 Velocity plot of 150W heater in zero gravity with magnet on with a) 20 A inner coil, 15 A outer coil b) 15 A inner coil, 10 A outer coil c) 10 A inner coil, 5 A outer coil

2.2.4 Earth Gravity with Magnet off vs Magnet on

Earth gravity simulation also showed the maximum system temperaure was the same in both cases after two mintues (Figure 2-10). Figure 2-10 shows the temperature in Kelvin with red being the highest temperature and blue the coldest. The combined convective case shows that the fluid movement causes more of the warmer fluid to move towards to the cooler bottom of the thruster than natural convection. Natural convection forces warm fluid up because it is less dense. In this simulation the warmer fluid was forced toward the heat source in the natural convective case, impeding heat transfer. The combined natural and thermomagnetic case shows that more warmer fluid was moved towards the bottom of the thruster helping with heat transfer.

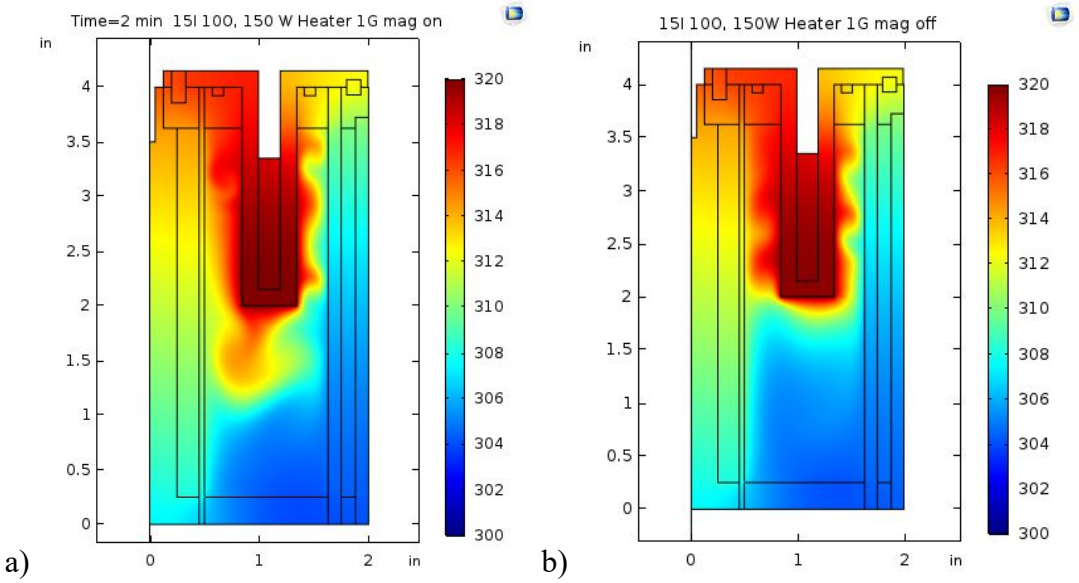

Figure 2-10 Temperature (K) plot of 150W heater with 15 A to the inner coil and 10 A to the outer coil in gravity with a) magnet on b) magnet off

Earth gravity simulations of pure natural **c**onvection (earth gravity, magnet off) and combined natural and thermomagnetic convection (earth gravity, magnet on) show the largest velocity in the combined convection case (earth gravity, magnet on) (Figure 2-11). The maximum velocity of the nautral convection is .041 m/s and the maximum velocity of combined thermomagnetic and nautral convection is .02 m/s (Figure 2-11). This was an expected reslut but is explained by the fact that thermomagnetic convection is causing the

fuild to move to lower portion of the cavity. Natural convection is casuing the fluid to move to the top portion of the caivty due to gravity and bouncy explain in chapter one. In the lower portion of the fluid cavity during natural convection (magnet off) there is little to no motion in the fluid in the middle. In the lower portion of the fluid cavity with combined natural and thermomagnetic convection there is motion in the middle of the cavity. This shows that more of the fluid is moving in combined natural and thermomagentic convection then in pure natural convection (Figure 2-11).

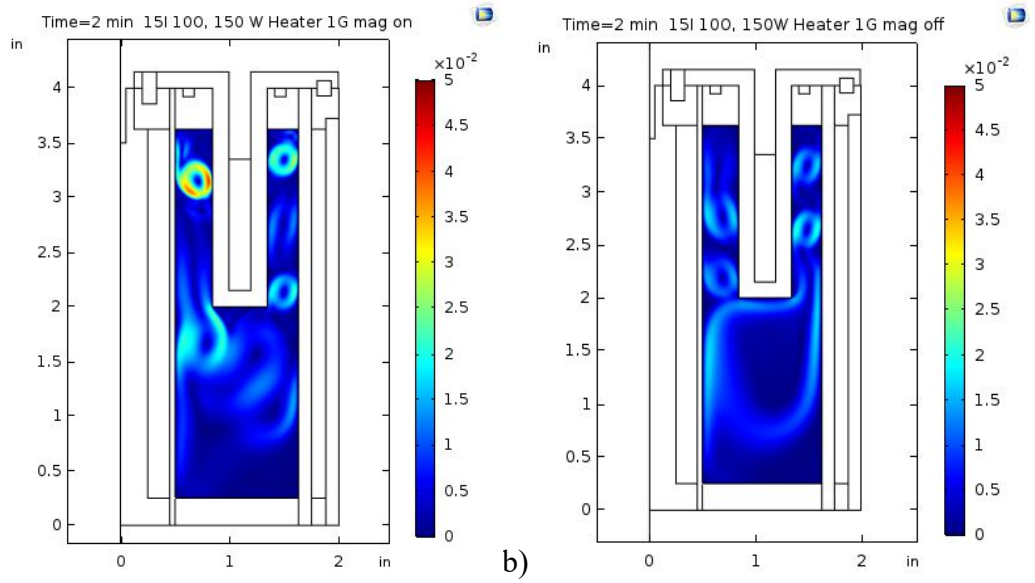

Figure 2-11 Velocity (m/s) plot of 150W heater with 15 A to the inner coil and 10 A to the outer coil in gravity with a) magnet on b) magnet off

Figure 2-12 shows that the direction of flow in natural convection in the sides of the cavity was up towards the heat source. The flow of the fluid during the combine

convections was overall weaker then natural convection, but the flow in the side of the cavity was down due to thermomagnetic convection.

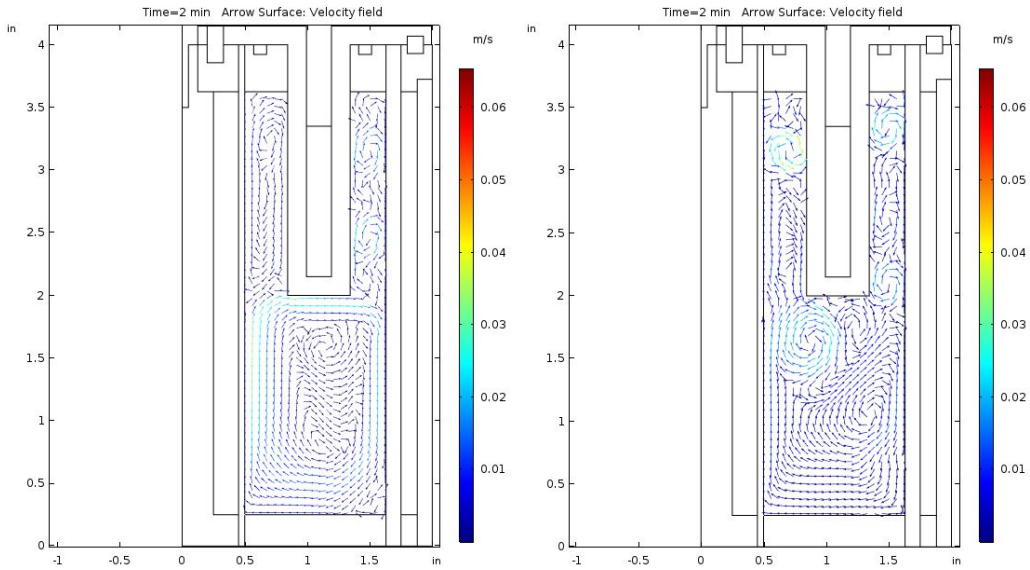

Figure 2-12 Velocity (m/s) arrow plot of 150W heater with 15 A inner coil, 10 A outer coil in a) earth gravity with magnet off b) earth gravity with magnet on

2.3 Conclusion of ILFF Numerical Results

The simulations showed that the cavity shape, location of the heat source and magnetic field will lead fluid motion under different gravity conditions and magnetic settings (Table 2-5). Thermomagnetic convection will cause the fluid to move differently than the natural convection case. The zero gravity cases showed that thermomagnetic convection will cause fluid motion at serval different magnetic settings, while conduction will cause no motion in the fluid in zero gravity. This shows that the proposed ferrofluid cavity could work in space.

Table 2-5 Summary of Numerical Simulations Results

Coil settings	Gravity settings	Magnet Setting	Velocity (m/s)
15 A inner coil 10 A outer coil	Earth Gravity	On	.02
		Off	.041
15 A inner coil 10 A outer coil	Zero-Gravity	On	.05
		Off	0

2.4 Modified EFH1 Ferrofluid

Currently Ionic Liquid Ferrofluids (ILFF) are being used by researchers to develop small satellite thrusters [36, 37]. Researchers developed this fluid initially for medical applications[11]. Due to the manufacturing and materials required to create an ILFF it is expensive. Due to the large quantity of fluid needed for the test thruster experimental tests were run with a modified Ferrotec EFH1 ferrofluid.

Unlike the ILFF, EFH1 has magnetite nanoparticles. EFH1 nanoparticles are easily produced, however EFH1 nanoparticles are not temperature sensitive. Ferrotec EFH1 ferrofluid is a fatty acid surfactant ferrofluid with an oil soluble dispersant. EFH1 has a boiling temperature of 496K (223ºC/433°F) and a high vapor pressure that led to outgassing in vacuum. This dispersant was replaced so the nanoparticles could be used in experimental testing to show that easily produced iron-based nanoparticles could be used for heat transfer applications with the right dispersant.

Dodecylbenzene was chosen as the new dispersant because of its lower vapor pressure and high boiling temperature of 561°K (288°C/550°F). Dodecylbenzene had prior success as a dispersant in a vacuum for an electrospray application. With a low vapor pressure, dodecylbenzene can maintain a liquid state at low pressure. Dodecylbenzene's boiling temperature was also higher than the original EFH1 dispersant, along with the low

vapor pressure this allowed for the experiments to reach closer to Curie temperatures while testing.

Since EFH1 nanoparticles are different from the ILFF, equation (2.1) becomes

$$M_d(T) = 13.72(1 - 3.01e^{-6}T^2) \tag{2.1}$$

Magnetite Fe_3O_4 Curie temperature is around 850 K (577ºC/1070ºF); however, due to the coating and the size of the particle, Ortega states that the Curie temperature of the bulk magnetite is lowed when the nanoparticles are created and coated with surfactant [27, 38]. According to Ortega's. in equation (2.1) the Curie temperature of nanoparticles is around 575K (Figure 2-13) [27].

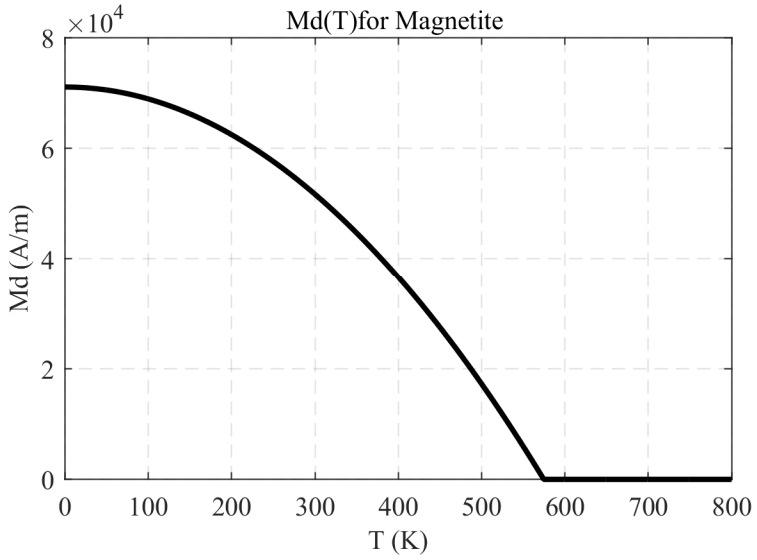

Figure 2-13 Magnetic saturation of the bulk magnetite particles

2.5 Modified EFH1 Numerical Simulation Results

Simulations were modified to see if the modified EFH1 would cool the test thruster (Figure 2-14). The earth gravity simulations show there is a noticed temperature difference between tests with natural convection and combined natural and thermomagnetic

convection with the modified EFH1 ferrofluid. Figure 2-14 is a snap shot of the temperature and velocity 30 minutes after turning on the heater. Due to low force on the fluid by the magnet there was only a maximum velocity of .00182 m/s with the magnet on. This lowed velocity and force by the magnet led to faster simulation times. Simulations with EFH1 in an earth gravity environment showed a velocity of .00182 m/s with the magnet on and of 0.00465 m/s with the magnet off. The maximum temperature with the magnet on was 500 K, and the maximum temperature with the magnet off was 554 K. This 54-degree temperature difference and strong magnetic field (650-700 Gauss in the gap of the annular channel) are ideal conditions for thermomagnetic convective cooling (Figure 2-14).

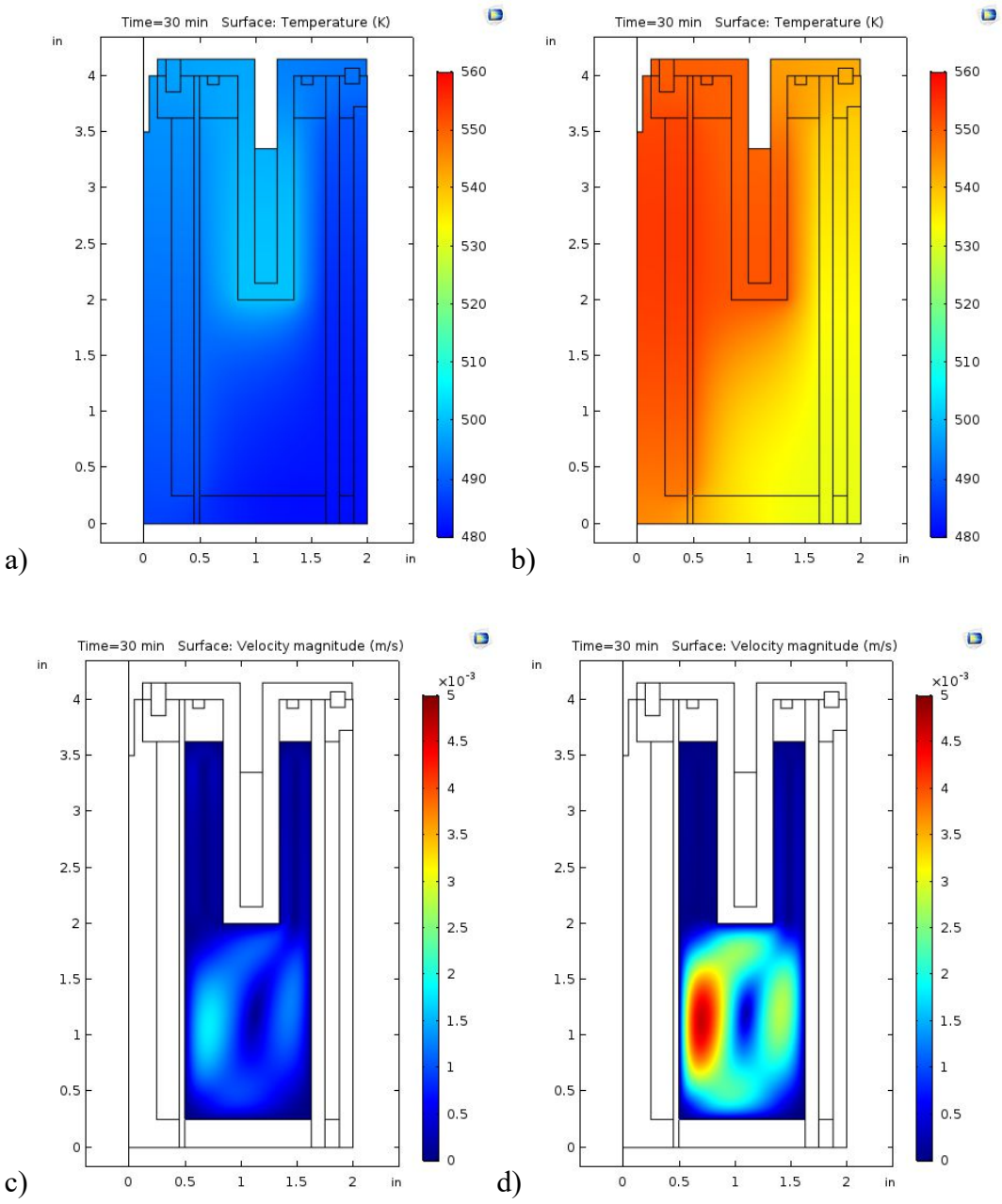

Figure 2-14 150W heater with 15 A to the inner coil power, 10 A to the outer coil. Thermal (K) picture of test device with EFH1 Mod2 with gravity and a) magnet on b) magnet off. Velocity (m/s) plot of test device with gravity and c) magnet on d) magnet off.

The above test shows after 30 minutes with the magnet on, the system achieved a lower maximum system temperature and a lower maximum velocity than natural convection (Figure 2-14). However, the expectation was that natural and thermomagnetic

convection fluid motion would combine and produce a higher velocity than just natural convection. Fluid motion in the natural convective case was concentrated in the lower portion of the fluid cavity. Figure 2-15 shows an arrow plot of the velocity magnitude and directions. In the combined convective case the fluid motion on the left-hand side of the cavity is stronger than the natural convective case and is also moving downward; this downward motion is counter to the motion in the bottom half of the cavity, this could slow down the motion within the bottom convective cell. In the natural convective case the fluid motion was upward; this could be a reason the bottom convective cell is stronger than the combined convective case.

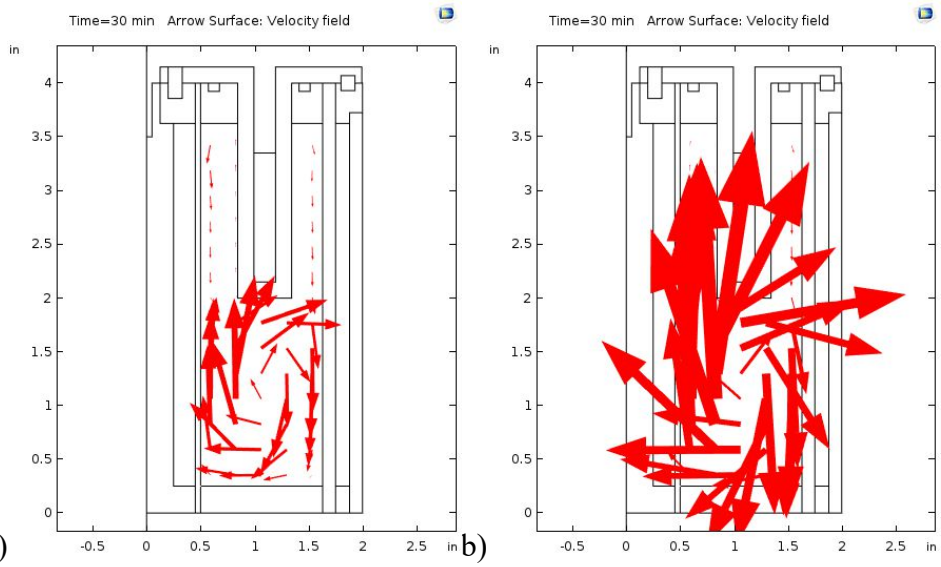

a) b)

Figure 2-15 Arrow surface of velocity magnitude and direction. a) magnet on b) magnet off

3 Experimental Testing

3.1 Test Thruster

The test thruster modeled the geometry and thermal attributes of a real Hall-effect thruster (HET) to validate the computational models described later in this chapter. This model was not meant to operate like an actual thruster. The test thruster was made of general purpose low carbon steel (Figure 3-1).

The steel components that made up the ferrofluid cavity were welded together to ensure a sealed cavity; this cavity is green in Figure 3-1. The remaining steel parts were spot-welded together. The blue top outer piece and purple top inner piece were spot-welded to the fluid cavity. The two electromagnetic coils are brown (Figure 3-1). The dark gray outer wall assembly was spot-welded together and slid in place after the coil was wrapped around the outside of the fluid cavity. The light gray piece is the inner core and was slid in place after the inner coil was wrapped around it. The inner core and outer wall assembly were held in place by the coils. The dark red piece is the copper top that replicated the channel of a Hall-effect thruster. The black piece in the middle of the thruster is the ferrofluid. The other two small black pieces near the copper top are the O-ring seals for the fluid cavity.

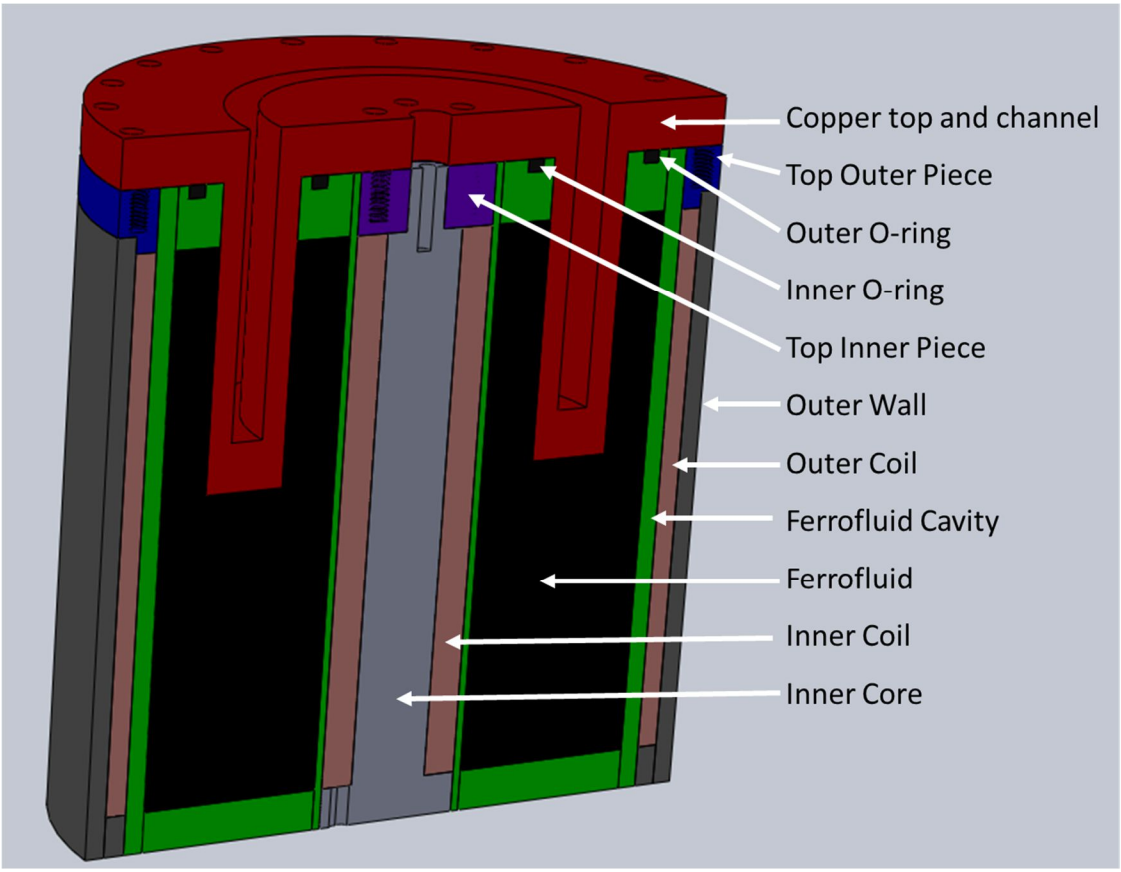

Figure 3-1 SolidWorks cross-section view of the test thruster

The coils are enamel coated copper wire. Each electromagnet coil had two layers. The electromagnets were counter wound so that the same power was put into the system while the electromagnets were not producing a magnetic field. In normal HETs a few hundred gauss was required in the channel for the thruster to operate [25].

The channel where the process occurs to create thrust was created within the copper top (Figure 3.2a and b). This was secured to the rest of the thruster by 20 outer screws and six inner screws that created the seal for the fluid cavity. In a typical HET, this would have been made of boron nitride to insulate the thruster and provide protection from ionic collisions that occur during operations. Copper simulated heat conduction that happens at high temperatures. The fluid cavity was sealed with two O-rings, a Viton inner seal and a Kalrez outer seal, between the copper channel and the top of the steel fluid cavity, (Figure 3-2c). The inner seal sees the highest temperature and required a more robust seal. The

fluid cavity was filled through two holes on the bottom of the devices. These holes were sealed with self-sealing hex bolts with Viton O-rings.

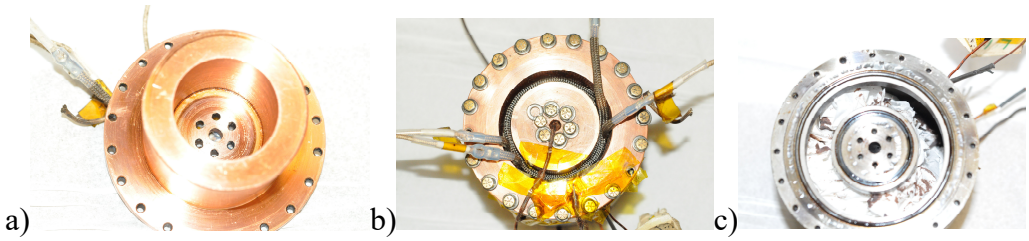

Figure 3-2 a) underside of the copper channel b) top view of copper channel c) top view of the fluid cavity with seals

A heater rope was wrapped around the channel created in the copper (Figure 3-2b). The heater rope is a current carrying wire that could produce its own magnetic field, to avoid this the rope was counter wrapped. The heater rope was later replaced with two heater ropes, counter wound to decrease the magnetic field produced by the ropes. The magnetic field produced by this setup was less than one gauss. This heater replicated heat created by the ionic reaction that occurs during normal operations of a HET.

Six K-type thermocouples were place on the test model to capture temperature throughout the device (Figure 3-3). These thermocouples where read by a data acquisition system and processed by LabView. Post processing was done in Matlab. Two thermocouples were placed near the inner coil on the fluid wall, one on top of the coil windings (Figure 3-4a). The outer coil thermocouple was placed underneath the coil touching the outside of the fluid wall. Another thermocouple was placed in a hole created on the top of the inner core to obtain the temperature near the critical part of the magnetic circuit (Figure 3-4b). This placement allowed for three measurements near the core, the location that is the hottest. Another thermocouple was placed on the bottom of the device located in between the two fluid walls (Figure 3-4c). The last thermocouple was placed near the outer edge of the copper top.

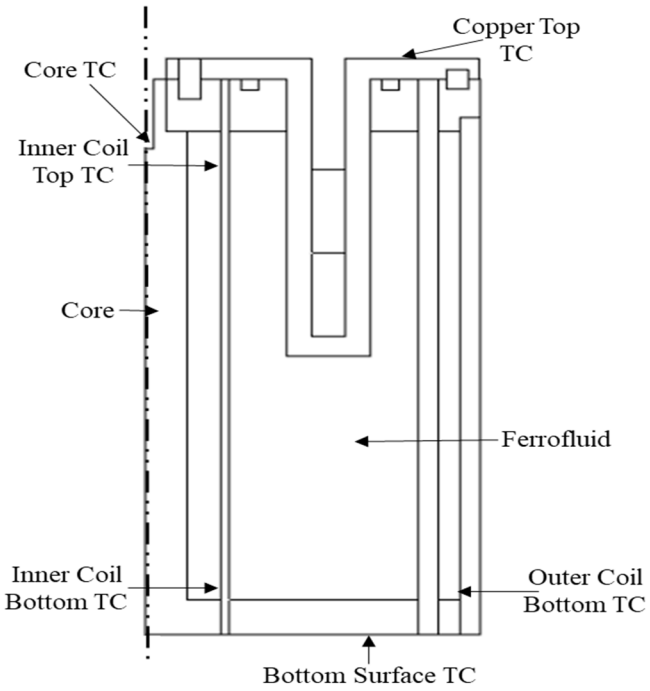

Figure 3-3 Axisymmetric drawing of the HET with thermocouple locations

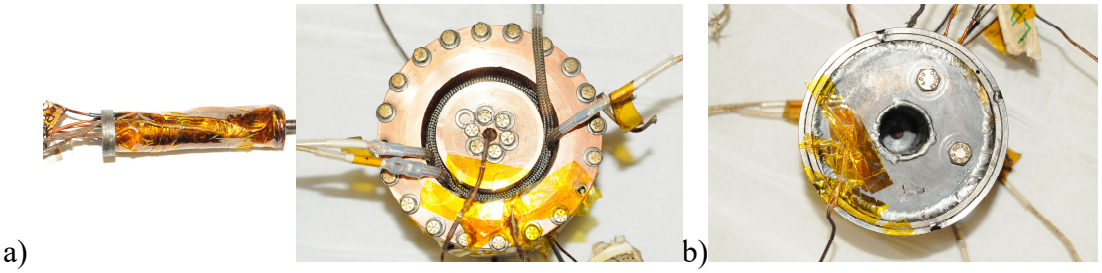

Figure 3-4 a) Inner coil thermocouples b) Top surface thermocouples c) Bottom surface thermocouple

The device was set up in the Condensable Propellant Facility at the Ion Space Proplusion Lab at Michigan Technological University (Figure 3 -5b). The annular channel was orientated towards the ceiling allowing for even distrubution of gravity within the fluid cavity from top to bottom. The device was not thermaly isolated; it was placed on two

pieces of unistruct which were in contact with the tank. The tank wall temperature was maintained at nearly room temperature.

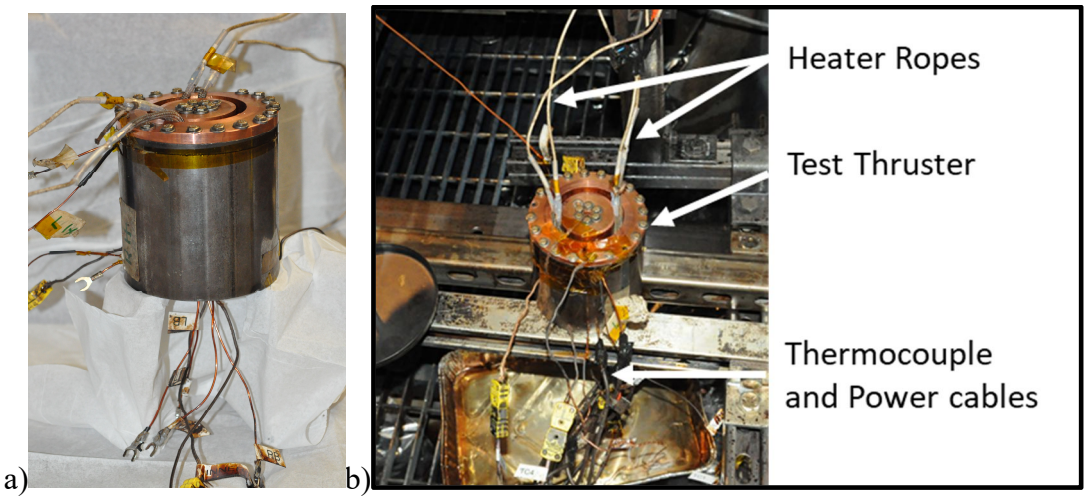

Figure 3-5 a) Assembled test thruster b) Test thruster setup in the Condensable Propellant Facility

3.2 Limitations of Modified EFH1 Ferrofluid

EFH1 Ferrofluid was modified to obtain a fluid that could withstand higher temperatures at vacuum. The carrier fluid of the EFH1 was evaporated which left a paste with trace amounts of the EFH1 dispersant, an oil-based fluid. The first ferrofluid mixture called, modification one (EFH1 Mod 1), was equal amounts of dodecylbenzene to equal amounts of EFH1 evaporated. This made the first mixture almost the same concertation of ferrofluid as the original EFH1, which was estimated at about 3-15% nanoparticles by volume. Another mixture was created with a 2.3g of EFH1 paste to 1 ml of Dodecylbenzene, making a second modification of EFH1 (EFH1 Mod 2). This second mixture was the highest concentration of nanoparticles that would maintain a viscous fluid and not form a paste that would impede fluid flow. The material properties of the EFH1 were modified due to the dodecylbenzene (Table 3-1).

Table 3-1 Material properties for test ferrofluid

Property	Dodecylbenzene	EFH1 Mod 1	EFH1 Mod 2	Units
Dynamic Viscosity	.009773 @273K* .002811 @322K	Eq. (1.16)	Eq. (1.16)	Pa*s
Ratio of specific heats	1	1	1	1
Density	900	1050**	1550**	Kg/m^3
Thermal Conductivity	.151049707*	.169 (see Eq. (1.17) and (1.18))	.2 (see Eq. (1.17) and (1.18))	W/(m*K)
Relative permeability	.9999992	Eq. (1.6)	Eq. (1.6)	1
Volume Fraction	0	.15	.5	1

*Cameo Chemicals https://cameochemicals.noaa.gov/chris/DDB.pdf

** Measured values, equation (1.19) for simulations

While conducting initial testing in the test thruster with 150W heater and 15 A to the inner coil and 10A to the outer coil the fluid seals would break. A volume expansion test of the dodecylbenzene was conducted. Multiple sources did not have all the material properties for dodecylbenzene, specifically volumetric expansion coefficient (Table 3-2). A volumetric expansion test was run with the EFH1 Mod 1. While heating the fluid at rough vacuum, the surface of the fluid was observed to have created a hard surface, the surface tension of the fluid increased to such an extent as to appear like a hard or sealed surface. Around 60°C a bubble broke through this hard surface, this buddle caused a sudden vaporization that shot ferrofluid more than four feet on to the vacuum chamber celling, no

expansion was observed. The bubble may have been trapped gas or the start of vaporization.

Table 3-2 Vapor Pressure of Dodecylbenzene

Source	Vapor Pressure (Pa)	Vapor Pressure (Torr)
ACD/Labs	0.0±39 Pa at 25ºC	0.0±0.3 Torr at 25ºC
EPISuite	0.0581 Pa at 25ºC	.000436 Torr at 25ºC
CAMEO Chemicals	28260.3465 Pa	211.97 Torr
HSDB	.006799 Pa at 25ºC	.000051 Torr at 25ºC
ILO-ICSC	<10 Pa at 20ºC	<.075 Torr at 20ºC

To determine the cause of the sudden vaporization at much lower temperatures than expected, a volume expansion test was run on the dodecylbenzene. Several sources stated different vapor pressures for dodecylbenzene (Table 3-2) [39, 40]. During the pressure decrease (pump down process) of the vacuum chamber the dodecylbenzene bubbled, as if to release all the gas trapped in the fluid (outgas). Once stable at rough vacuum the test showed that the dodecylbenzene boiled at 110℃ at a pressure of 200 mTorr. The test also showed that the fluid only expanded by 2.5%by volume throughout the test.

A volumetric expansion test of EFH1 Mod 2 showed that the ferrofluid initially bubbled like dodecylbenzene while pumping down to rough vacuum. During the heating process, the ferrofluid boiled obscuring the view of the volume, no expansion could be

observed. EFH1 Mod 2 however did not suddenly vaporize like EFH1 Mod 1, rather the dodecylbenzene evaporated leaving the nanoparticles and little fluid.

Boiling occurs when the vapor pressure above the fluid is the same as the fluid. For test conducted with pure dodecylbenzene, the fluid boiled at 110ºC at 200 mTorr. The Clausius-Clapeyron equation relates vapor pressure to temperature.

$$P(T_1) = \frac{P(T_0)}{e^{\frac{\Delta H}{R} * \left(\frac{1}{T_1} - \frac{1}{T_0}\right)}} \tag{3.1}$$

Using this equation, we can now find the vapor pressure at any temperature. T_1 is the temperature we are trying to find the vapor pressure at P(T_1), $T_0$is the initial temperature. We also know the vapor pressure at room temperature P(T_0). R is the gas constant at 8.315 J/(K*mol) and ΔH is the enthalpy of vaporization at 55,100 J/mol.

Using equation (3.1) and published vapor pressures (Table 3-2) figure (3-6) shows a plot of the published value vapor pressures versus temperature. If the tested dodecylbenzene vaporized at 110ºC at 200 mTorr the calculated vapor pressure would have been around .0014 torr, the dash dot line in figure 3-6 shows this calculated value from the dodecylbenzene test. The closest published vapor pressure value to that of the tested fluid is .000436 torr, meaning that the tested fluid was .000264 torr larger, a 45% error.

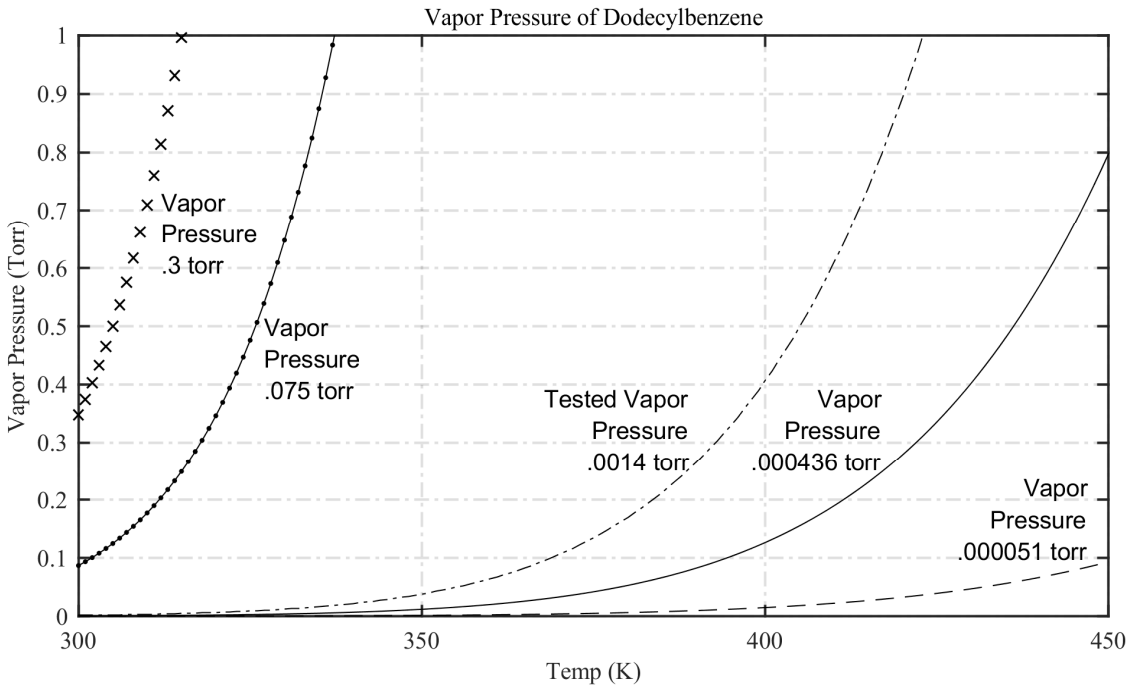

Figure 3-6 Vapor pressure of dodecylbenzene

The cause of the sudden vaporization in the EFH1 Mod 1 could be due to the uncertainty of the vapor pressure. The sudden vaporization could have also been caused by the additions of the EFH1 nanoparticles and the trace amounts of the oil-based dispersant could have also cause the decreased vapor pressure of the fluid. Due to the nonlinear volumetric expansion test of EFH1 Mod 1, experimental test were limited to maximum temperature of no more than 60ºC.

3.3 Experiment Results

Two identical tests with the conditions above of a 15W heater, 8 A to the inner coil producing 45W of power, and 6 A to the outer coil producing 33W of power for a total power input of 93W were run. This is different from the simulation above because of the length of wire leading into the coils. In the experimental setup this additional wire adds resistance and increases the power needed by $\pm$5 watts.

Figure 3-7 shows individuals plots for each thermocouple. This test shows the top of the inner core is the hottest part of the thruster. The inner coil temperatures are similar as they are both located on the coil. The thermocouple on the top of the inner core is the next hottest temperature. This means that test conditions are similar to thermal conditions that occur during thruster's operations.

This test also shows that the predicted 18-degree temperature difference between the top and bottom of the thruster is 30°C. One reason for this is the ideal mating that occurs in the simulations. COMSOL assume no air gaps or rigid surface that occur in the real-world surface matting. Another reason for the large difference in predicted temperatures is that one of the boundary conditions in the simulations maybe slightly off the real-world properties. For example, the dynamic viscosity of the fluid is computed using the equations in chapter one, but the actual fluid viscosity could be quite different.

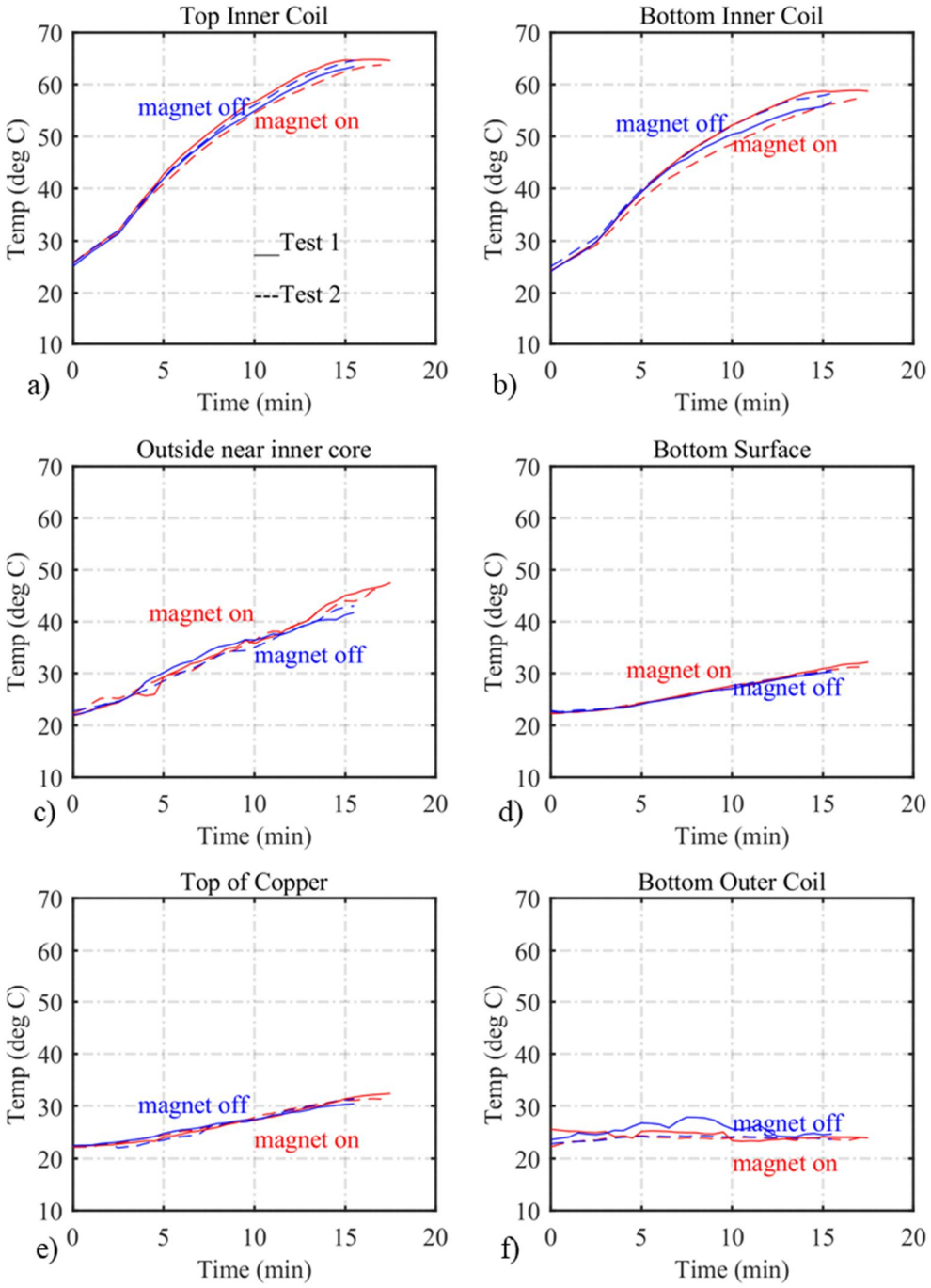

Figure 3-7 15W heater, 8 A inner Coil, 6 A outer coil, EFH1 Mod 2 ferrofluid. a) top inner coil thermocouple b) bottom inner coil thermocouple c) outside inner core thermocouple d) bottom surface thermocouple e) top copper thermocouple f) bottom outer coil thermocouple

Thermocouples are accurate within $\pm$1.5 degrees. Thermocouples also have noisy signals, which is made worse by the length of wire the signal is transmitted through. This noise increased the error of the thermocouple to 2-3 degrees. The wire length could not be shortened and the location of the test thruster in the tank was optimal for running multiples test.

Several different tests were run with different current to the coils, which varied the magnetic field strength, different heater power setting, and two different concentrations of fluid. All the variations had the same result; little to no noticeable difference between the magnet on and the magnet off (Table 3-3). Coil settings of 10 A for the inner coil and 8 A for the outer coil was the maximum setting that allowed for more than five minutes of testing before reaching 60°C. Each test showed that the magnet on and the magnet off were within 1.5 to 3 degrees of each other.

Table 3-3 Summary of Test

Current to outer Coil (A)	Current to inner Coil (A)	Magnetic Field (G)
10	8	160
8	6	144
6	4	120
4	2	98
2	1	55

These tests did not show whether thermomagnetic convection occurred or not. If thermomagnetic convection occurred, it did not have a large enough temperature difference or magnetic field to produce an enhancement in heat transfer that was greater than natural

convection. There was no designed capability to measure the velocity within the ferrofluid cavity.

The initial test had the test thruster with the channel pointed towards the celling. Several tests were conducted with the channel pointed down. This was to see if natural convection was hindering the thermomagnetic convection or the position of the heat source was in the wrong location as discussed in Bohzo research in chapter one [19, 27]. These tests did not show any noticeable difference from pervious test (Figure 3-8). This test is like the previous test results.

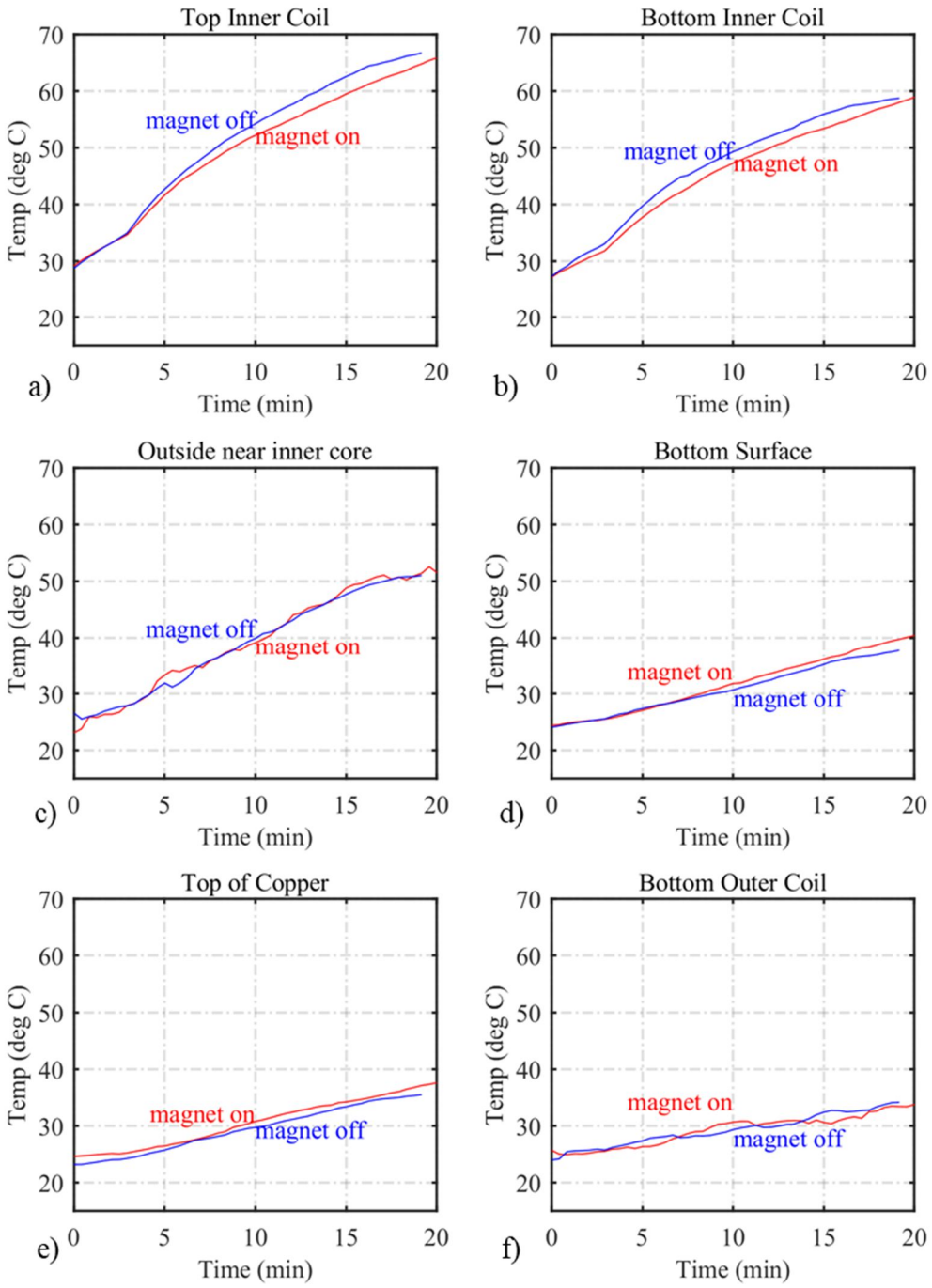

Figure 3-8 15W heater, 8 A inner coil, 6 A outer coil, EFH1 mod 2 ferrofluid, test thruster pointed down. a) top inner coil thermocouple b) bottom inner coil thermocouple c) outside inner core thermocouple d) bottom surface thermocouple e) top copper thermocouple f) bottom outer coil thermocouple

The bottom outer coil temperature is warmer then the upright test (Figure 3-7 and 3-8). This occurred because of the orientation of the thruster. The outer coil thermocouple was located on the bottom on the thruster. In the upright test the warm fluid was forced toward the heat source due to gravity. In the downward pointing case, the warmer fluid was forced toward the bottom of the thruster and away from the heat source. The downward orientation did not show that thermomagnetic convection was hindered.

As stated above in chapter one, research indicated that the magnetic field and the temperature gradient had to be large enough to see the onset and the dominance of thermomagnetic convection. Due to the limitation of the modified ferrofluid in this test setup it did not allow thermomagnetic convection to dominate the convective cell and did not enhance heat transfer.

4 Analysis and Conclusion

A Hall-effect thruster's magnetic circuit must be kept cool and under the Curie temperature for the thruster to operate. Recent research shows that the hottest component of the thruster is near the top of the inner core. Recent research has attempted to cool the thruster by adding additional heats sinks. This study attempted to cool this component with a ferrofluid cavity designed to fit in an existing void in the thruster.

Roissenwieg developed an equation for the force the magnet applies to the nanoparticles within the fluid, known as the body force (1.1)(1.12)(1.13). However, the magnetic saturation of the nanoparticles is different than the bulk magnetic material because of the surfactant coating as show by Orteag. This difference resulted in a temperature dependent equation for both magnetic saturation and magnetization of the fluid, creating a body force equation with a complex temperature dependence and magnetic field strength dependence.

Hall Effect thrusters reach temperature around 900K. Iron oxide and other derivations have been used in ferrofluids, iron oxide particles are easy to produce nanoparticles and have a curie temperature around 700 K. However, the typical fluid used for dispersants have a decomposition temperature much lower than 700 K. Ionic liquid decomposition temperature is near 700 K. Using ionic liquids in ferrofluids allows the use of iron oxide nanoparticles and the ability to obtain a ferrofluid with an overall higher curie temperature. This higher temperature allows the nanoparticles to reach a point where there is a significant difference in magnetic susceptibility that occurs near the Cure temperature of the nanoparticles. The advantage of allowing the temperature of the fluid to reach near the Curie temperature is that there is a greater effect form thermomagnetic convection as discussed in chapter one.

This study showed numerically, using COMSOL Multiphysics, that a Hall-Effect thruster could potential be cooled with the designed ferrofluid cavity in zero gravity conditions using an Ionic Liquid Ferrofluid (ILFF). Simulations show that in zero gravity conditions within the first two minutes of heating thermomagnetic convection creates

motion in the cavity. Due to the limited duration of the simulation it did not show a temperature difference between simulations without the thermomagnetic effect, pure conduction, and thermomagnetic convection.

ILFFs are not easy to produce and are thus very expensive. Due to the amount needed to fill the cavity an alternative ferrofluid was used for testing. EFH1 dispersant was replaced with dodecylbenzene, to replicate ILFF properties. The volume expansion test of the modified EFH1 showed that the ferrofluid could not withstand temperatures of more than 60ºC. The magnetic field and heater power were lowered due to above stated temperature limitation of 60ºC.

Refined simulations show thermomagnetic convection occurred with that limitations. Figure (4-1) shows the maximum temperature with the magnet on was 331 K and with the magnet off was 349 K. Figure (4-1) also shows that the low magnetic field and low heater power resulted in an 18 Kelvin temperature difference. Research discussed in chapter one has shown that thermomagnetic convection can occur with only an 18 Kelvin temperature difference and less.

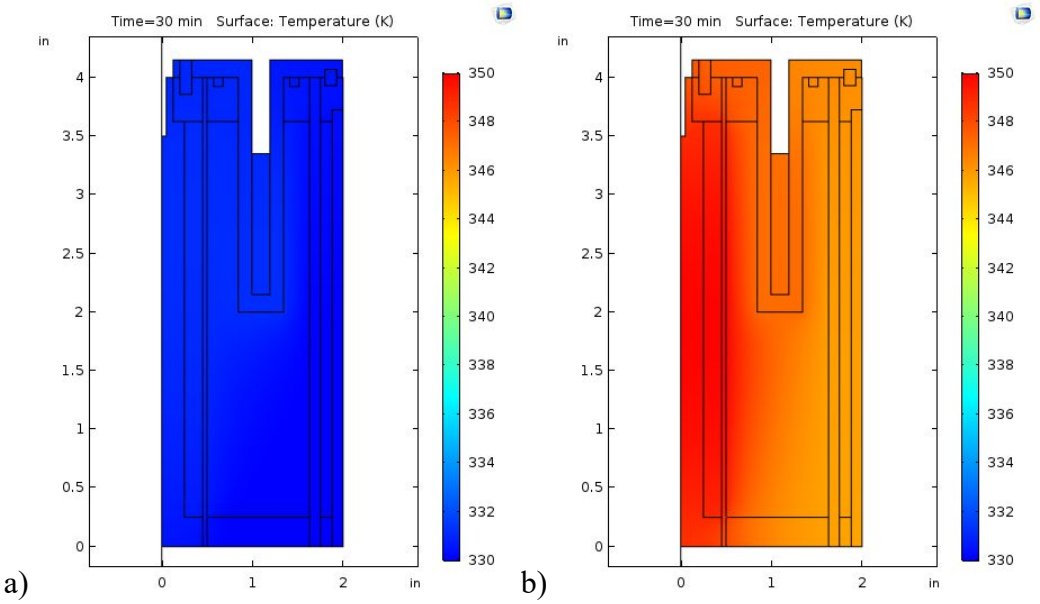

Figure 4-1 Thermal plot with 15W heater, 8 A to the inner coil and 4 A to the outer coil with gravity and a) magnet on b) magnet off.

The velocity of the fluid under the influence of both gravity and the magnetic body force in Yang's papers, discussed in chapter one, was .01 m/s (10mm/s). For the earth gravity simulations with EFH1 Mod 2, the maximum velocity with the magnet on was .00027 m/s (.27 mm/s) and with the magnet off was .00125 m/s (.125 mm/s) (Figure 4-2). The velocity with the EFH1 Mod 2 showed a much lower velocity.

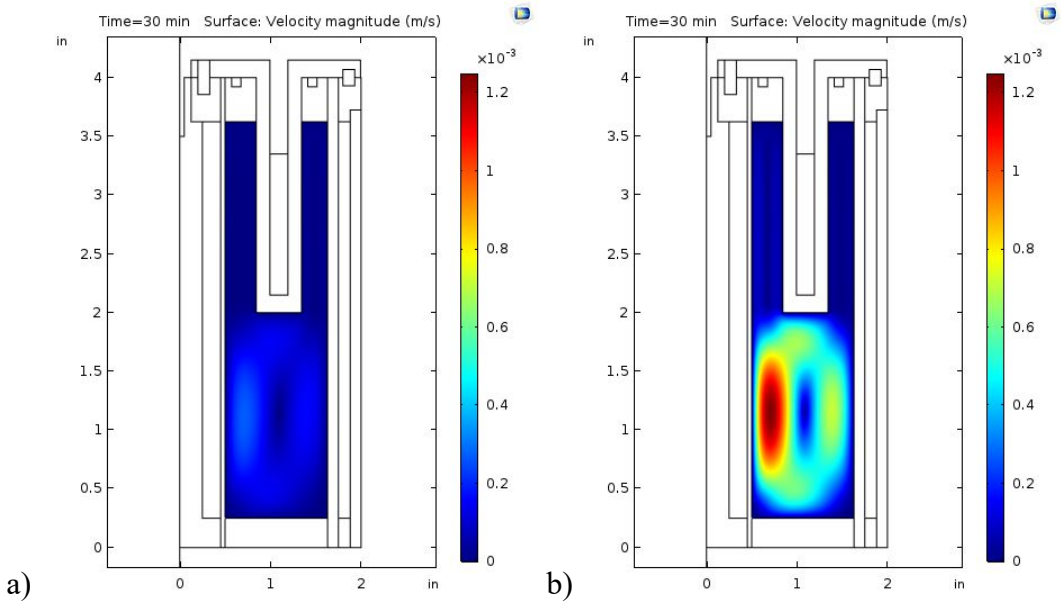

Figure 4-2 Velocity plot of test conditions of 15W heater, 6 A inner 4 A outer coil with gravity and a) magnet on b) magnet off.

The refined EFH1 Mod 2 simulations show the natural convective cell is concentrated on the bottom of the fluid cavity. As discussed above, thermomagnetic convective cells are moving in the opposite direction of natural convection and reducing the velocity of the convective cell in the combined convective case. The natural convective case seems to be concentered near the bottom of the inner coil. In this setup the power in the inner coil is 23 W which is almost double the power of the 15 W heater. The velocity is lowered in the combined convective case and which could mean that thermomagnetic convection is slowing the natural convective cell down as discussed in the simulations results section of chapter two (Figure 4-3).

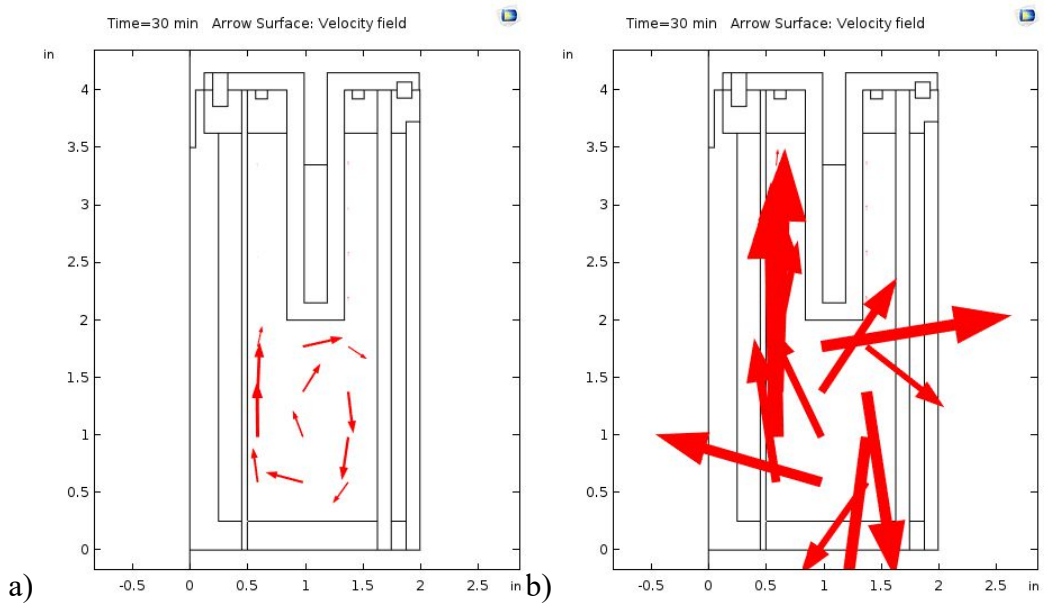

Figure 4-3 Arrow surface of the velocity magnitude and directions a) magnet on b) magnet off

There are also three heat sources in test thruster, the two electromagnets and the heat source in the channel. Under the above simulation conditions, there is 23W and 17W of power input form the inner and outer coil respectively and 15W of power for the heater for 55W of power for the system. The power in the inner coil is more than the heater, which seems to have increased the convective currents in the bottom region of the thruster.

The magnetic field strength at these settings in the gap of the annular channel was at a maximum of 500 Gauss. The temperature difference as seen from the simulation is only 18 Kelvins. According to previously discussed research and the above simulations, the temperature difference is large enough to induce thermomagnetic convection, but not large enough for maximum effectiveness of thermomagnetic convection for heat transfer.

However, experimental test did not show that thermomagnetic convection was dominate or that it even occur. Experiments were run with a modified simple ferrofluid. This modification was meant to decrease the vapor pressure and increase the fluids ability to withstand heat. Testing of the modified fluid showed unpredicted boiling temperature at

rough vacuum of 60°C. Simulations showed an 18 Kelvin difference, however experiments with the modified fluid did not show results of an enhancement of heat transfer.

The Curie temperature of magnetite is 858K (585°C) or 575K (301°C) and the boiling point of dodecylbenzene is 561K (288ºC). The operating temperature at the lower power settings does not allow for a large difference in magnetic susceptibility. To have the greatest difference in magnetic susceptibility, the Curie temperature of nanoparticles need to be lower than boiling temperature of the fluid. Upadhyay synthesized a temperature sensitive ferrofluid with Curie temperature around 340K (66ºC) [30]. For application in a HET with maximum operating temperature around 800K, having a ferrofluid with a Curie temperature around 810K would be optimal. These experiments further prove that ILFFs are ideal for this application.

Ferrofluid designs has room for further exploration. The nanoparticles, surfactant and dispersant. The nanoparticles should be chosen so that the curie temperature of the particles with the surfactant coating is near the maximum temperature of the application. The dispersant then needs to be choose so that the break down temperature is higher than the Curie temperature of the nanoparticles. Iron oxide nanoparticles are easy to produce and have a high Curie temperature. The ferrofluid than needs to be tested to ensure a stable ferrofluid. The experimental dispersant in this study did not behave how it was expected to with the addition of the nanoparticles and resulted low temperature tolerance.

Recent trends in Hall effect thruster research has been studies on making them smaller and more efficient. With this trend further research on cooling the thruster should be conducted with miniature thruster. This would allow for the use of ILFF.

Thermomagnetic convection has numerical shown to induce motion within the fluid and move heat away from the hottest part of a Hall-effect thruster with a cavity designed within the existing void of the thruster. This study did not show or prove that this application works experimentally.

5 References

[1] P. S. Stephen, "Low Viscosity Magnetic Fluid Obtained by the Colloidal Suspension of Magnetic Particles," ed: Google Patents, 1965.

[2] N. Technology. (2015) Magnetic Fluids Deliver Better Speaker Sound Quality. *Consumer Goods* Available: https://spinoff.nasa.gov/database/spinoffDetail.php?this=/spinoff//grc/GRC-SO-208

[3] C. Scherer and A. M. F. Neto, "Ferrofluids Properties and Applications," *Brazilian Journal of Physics,* vol. 35, no. 3A, pp. 718-728, 2005.

[4] J. Singh Mehta, R. Kumar, H. Kumar, and H. Garg, "Convective Heat Transfer Enhancement Using Ferrofluid: A Review," *Journal of Thermal Science and Engineering Applications,* vol. 10, no. 2, 2017.

[5] P. Zohrabi, M. Shamsipur, M. Hashemi, and B. Hashemi, "Liquid-Phase Microextraction of Organophosphorus Pesticides Using Supramolecular Solvent as a Carrier for Ferrofluid," *Talanta,* vol. 160, pp. 340-346, 2016.

[6] B. S. P. a. Systems. (8 March 2018). *First US Hall Thruster in Space, TACSAT-2 (Launched 2006, Success)*.

[7] B. S. P. a. Systems. (2012). *Busek's Hall Effect Thruster Technology Saves Air Force AEHF Satellite*.

[8] R. W. Conversano, D. M. Goebel, R. R. Hofer, T. S. Matlock, and R. E. Wirz, "Magnetically Shielded Miniature Hall Thruster: Development and Initial Testing," in *Proceedings of the thirty-third international electric propulsion conference, Electric Rocket Propulsion Society, Washington DC, USA*, 2013.

[9] F. R. Viral K. Patel, Jamal Seyed-Yagoobi, Senior Member, IEEE, and Jeffrey Didion, "Terrestrial and Microgravity Experimental Study of Microscale Heat-Transport Device Driven by Electrohydrodynamic Conduction Pumping," *IEEE Transcations on Inductry Applications,* vol. 49, no. 6, p. 4, 2013.

[10] J. W. Tomaszewski, "Characterization of a Hall Effect Thruster using Thermal Imaging," Master of Science in Astronautical Engineering, Department of Aeronautics and Astronautics, Air Force Institues of Technology, 2007.

[11] N. Jain, X. Zhang, B. S. Hawkett, and G. G. Warr, "Stable and Water-Tolerant Ionic Liquid Ferrofluids," *ACS Applied Materials & Interfaces,* vol. 3, no. 3, pp. 662-667, 2011.

[12] M. Hadavand and A. Sousa, "Simulation of Thermomagnetic Convection in a Cavity Using the Lattice Boltzmann Model," *Journal of Applied Mathematics,* vol. 2011, 2011.

[13] M. Ashouri, B. Ebrahimi, M. Shafii, M. Saidi, and M. Saidi, "Correlation for Nusselt Number in Pure Magnetic Convection Ferrofluid Flow in a Square Cavity by a Numerical Investigation," *Journal of Magnetism and Magnetic Materials,* vol. 322, no. 22, pp. 3607-3613, 2010.

[14] M. T. Krauzina, A. A. Bozhko, P. V. Krauzin, and S. A. Suslov, "The Use of Ferrofluids for Heat Removal: Advantage or Disadvantage?," *Journal of Magnetism and Magnetic Materials,* vol. 431, pp. 241-244, 2017.

[15] R. R. Hofer, "Development and Characterization of High-Efficiency, High-Specific Impulse Xenon Hall Thrusters," Doctor of Philosophy, Aerospace Engineer, Univeristy of Michigan, 2004.

[16] S. Banerjee, A. Mukhopadhyay, S. Sen, and R. Ganguly, "Thermomagnetic Convection in Square and Shallow Enclosures for Electronics Cooling," *Numerical Heat Transfer, Part A: Applications,* vol. 55, no. 10, pp. 931-951, 2009.

[17] S. Mojumder, K. M. Rabbi, S. Saha, M. N. Hasan, and S. C. Saha, "Magnetic Field Effect on Natural Convection and Entropy Generation in a Half-Moon Shaped Cavity with Semi-Circular Bottom Heater Having Different Ferrofluid Inside," *Journal of Magnetism and Magnetic Materials,* vol. 407, pp. 412-424, 2016.

[18] S. M. S. S. S. S. M. A. H. Mamun, "Effect of Magnetic Field on Natural Convection in a C-Shaped Cavity Filled with Ferrofluid," presented at the 6th BSME International Conference on Thermal Engineering, 2014.

[19] A.Bozhko, Yu.Bratuhin, and G. Putin, "Experiments on Ferrofluid Convection in a Spherical Cavity," presented at the 15th Riga and 6th PAMIRConference on Fundamental and Applied MHD, Rigas Jurmala 2005.

[20] Q. Li and Y. Xuan, "Experimental Investigation on Heat Transfer Characteristics of Magnetic Fluid Flow Around a Fine Wire Under the Influence of an External Magnetic Field," *Experimental Thermal and Fluid Science,* vol. 33, no. 4, pp. 591-596, 2009.

[21] M. Goharkhah, "Application of Ferrofluid for Convective Heat Transfer Enhancement in Micro Gravity Conditions," presented at the 16th International Conference of Iranian Aerospace Society, Tehran, 2017.

[22] Y. Sheikhnejad, R. Hosseini, and M. Saffar Avval, "Experimental Study on Heat Transfer Enhancement of Laminar Ferrofluid Flow in Horizontal Tube Partially Filled Porous Media Under Fixed Parallel Magnet Bars," *Journal of Magnetism and Magnetic Materials,* vol. 424, pp. 16-25, 2017.

[23] M. Yang, R. O'Handley, and Z. Fang, "Modeling of Ferrofluid Passive Cooling System," in *Proc. of the COMSOL Conference*, pp. 1-6.

[24] M. Sheikholeslami and M. Gorji-Bandpy, "Free Convection of Ferrofluid in a Cavity Heated from Below in the Presence of an External Magnetic Field," *Powder Technology,* vol. 256, pp. 490-498, 2014.

[25] E. Kurtoğlu, A. Kaya, D. Gözüaçık, H. F. Y. Acar, and A. Koşar, "Experimental Study on Convective Heat Transfer Performance of Iron Oxide Based Ferrofluids in Microtubes," *Journal of Thermal Science and Engineering Applications,* vol. 6, no. 3, p. 7, 2014.

[26] M. Goharkhah, A. Salarian, M. Ashjaee, and M. Shahabadi, "Convective Heat Transfer Characteristics of Magnetite Nanofluid Under the Influence of Constant and Alternating Magnetic Field," *Powder Technology,* vol. 274, pp. 258-267, 2015.

[27] D. Ortega *et al.*, "Size and Surface Effects in the Magnetic Properties of Maghemite and Magnetite Coated Nanoparticles," *Philosophical Transactions of*

the Royal Society of London A: Mathematical, Physical and Engineering Sciences, vol. 368, no. 1927, pp. 4407-4418, 2010.

[28] L. Zhuang, W. Zhang, Y. Zhao, D. Li, W. Wu, and H. Shen, "Temperature Sensitive Ferrofluid Composed of Mn1−xZnxFe2O4 Nanoparticles Prepared by a Modified Hydrothermal Process," *Powder Technology,* vol. 217, pp. 46-49, 2012.

[29] T. Y. Chong, K. L. Ho, and B. H. Ong, "Investigations of Field Instability of Ferrofluid in Hypergravity and Microgravity," *AIP Advances,* vol. 2, no. 1, 2012.

[30] S. Odenbach, "Microgravity Experiments on Thermomagnetic Convection in Magnetic Fluids," *Journal of Magnetism and Magnetic Materials,* vol. 149, p. 3, 1995.

[31] S. A. Suslov, A. A. Bozhko, and G. F. Putin, "Non-Conducting Magnetic Fluids and their Application for Heat Removal in Micro-Gravity Conditions," 2009.

[32] R. E. Rosensweig, *Ferrohydrodynamics*, 2 ed. Courier Corporation, 2013.

[33] S. Genc, "Heat Transfer of Ferrofluids," in *Nanofluid Heat and Mass Transfer in Engineering Problems*, 2017.

[34] D. D. G. Mohsen Sheikholeslami, "Ferrohydrodynamic and Magnetohydrodynamic Effects on Ferrofluid Flow and Convective Heat Transfer," *Energy,* vol. 75, pp. 400-410, 2014.

[35] O. O. a. S. K. Banerjee, "High Temperature Stability of Maghemite," *Geophysical Research Letters,* vol. 11, no. 3, pp. 161-163, March 1984.

[36] K. J. Terhune, "Influence of Magnetic Nanoparticles and Magnetic Stress on an Ionic Liquid Electrospray Source" Doctor of Philosophy Mechanical Engineering Michigan Technological University Michigan Technological University Digital Commons, 2017.

[37] E. J. M. IV, "Development of an Ionic Liquid Ferrofluid Electrospray Source and Mode Shape Studeis of a Ferrofluid in a Non-uniform Magnetic Field," Doctor of Philosophy, Mechanical Engineering Michigan Technological University 2014.

[38] Y. D. Z. Mingzhoug Wu, S. Hui, T.D. Xiao, Shihui Ge, W.A. Hines, J.I. Budnick, "Temperature Dependence of Magnetic Properties of SiO20 Coated

Nanoparticles," *Journal of Magnetism and Magnetic Materials,* vol. 268, no. 2004, pp. 20-23, 2003.

[39] N. U. S. N. L. o. Medicine. (15 March 2018). *Phenyldodecane*. Available: https://pubchem.ncbi.nlm.nih.gov/compound/31237#section=Spectral-Properties

[40] R. S. o. Chemistry. (2015, 15 March 2018). *Dodecylbenzene*. Available: http://www.chemspider.com/Chemical-Structure.28977.html